Proposal for a Full-Scale Detector Engineering Test and Test Beam Calibration of a Single-Phase LAr TPC

A. name1[1], B. name2[2], and C. name3[3]

[1]Department of X1, University Y1
[2]Department of X2, University Y2
[3]Department of X3, University YY3

April 30, 2015

Abstract

After a short introduction to the ELBNF physics program we motivate the proposed single phase liquid argon detector and charged particle beam measurement program. We describe the required beam line and beam monitoring instrumentation for the project. The proposed single phase liquid argon detector presently described corresponds to the LBNE detector design. Discussions about alternate designs are in progress and this proposal will be updated according to a developing consensus on the detector design. The detector will be placed inside a membrane cryostat which will be connected to a cryogenics systems for which we provide engineering details. The proposal concludes with a description of data handling and analysis plans, as well as a schedule and an overview of the organizational structure put in place to execute the plan.

Contents

1 Introduction [~5 pages; Thomas/Greg/B.Wilson]

The preponderance of matter over antimatter in the early Universe, the dynamics of the supernova bursts that produced the heavy elements necessary for life and whether protons eventually decay - these mysteries at the forefront of particle physics and astrophysics are key to understanding the early evolution of our Universe, its current state and its eventual fate. The Experiment at the Long-Baseline Neutrino Facility (ELBNF) represents an extensively developed plan for a world-class experiment dedicated to addressing these questions.

Experiments carried out over the past half century have revealed that neutrinos are found in three states, or flavors, and can transform from one flavor into another. These results indicate that each neutrino flavor state is a mixture of three different nonzero mass states, and to date offer the most compelling evidence for physics beyond the Standard Model. In a single experiment, ELBNF will enable a broad exploration of the three-flavor model of neutrino physics with unprecedented detail. Chief among its potential discoveries is that of matter-antimatter asymmetries (through the mechanism of charge-parity violation) in neutrino flavor mixing - a step toward unraveling the mystery of matter generation in the early Universe. Independently, determination of the unknown neutrino mass ordering and precise measurement of neutrino mixing parameters by ELBNF may reveal new fundamental symmetries of Nature.

Grand Unified Theories, which attempt to describe the unification of the known forces, predict rates for proton decay that cover a range directly accessible with the next generation of large underground detectors such as the ELBNF detector. The experiment's sensitivity to key proton decay channels will offer unique opportunities for the ground-breaking discovery of this phenomenon.

Neutrinos emitted in the first few seconds of a core-collapse supernova carry with them the potential for great insight into the evolution of the Universe. ELBNF's capability to collect and analyze this high-statistics neutrino signal from a supernova within our galaxy would provide a rare opportunity to peer inside a newly-formed neutron star and potentially witness the birth of a black hole.

To achieve its goals, ELBNF is centered around three central components: (1) a new, high-intensity neutrino source generated from a megawatt-class proton accelerator at Fermi National Accelerator Laboratory (Fermilab), (2) a fine-grained near neutrino detector installed just downstream of the source, and (3) a massive liquid argon (LAr) time-projection chamber (TPC) deployed as a far detector deep underground at the Sanford Underground Research Facility (SURF). This facility, located at the site of the former Homestake Mine in Lead, South Dakota, is ~1,300 km from the neutrino source at Fermilab - a distance (baseline) that delivers optimal sensitivity to neutrino charge-parity symmetry violation and mass ordering effects. This ambitious yet cost-effective design incorporates scalability and flexibility and can accommodate a variety of upgrades and contributions.

ELBNF plans to place modular LAr TPCs with a combined total fiducal mass of at least 40 kton in the underground facility at Homestake and into the neutrino beam. The first 10 kton LAr TPC module is planned to be constructed underground on the time scale of 2021.

With its exceptional combination of experimental configuration, technical capabili-

ties, and potential for transformative discoveries, ELBNF promises to be a vital facility for the field of particle physics worldwide, providing physicists from institutions around the globe with opportunities to collaborate in a twenty to thirty year program of exciting science.

1.1 Key physics goals of ELBNF

The primary goal of ELBNF is to measure the appearance of electron neutrinos in a beam of muon neutrinos and and the appearance of electron anti-neutrinos in a beam of muon anti-neutrinos, each over the 1300 km baseline of the experiment. Precise measurement of this phenomenon would allow for determination of the relative masses and mass ordering of the three known neutrinos. Measurement of these neutrino oscillation channels also allow to constrain or measure the CP violation phase, δ_{CP} in the neutrino sector, which is possibly connected to the dominance of matter over antimatter in the universe.

For a baseline of 1300 km the first maximum of the oscillation probability occurs in the 2 - 3 GeV energy range with additional oscillation maxima at lower energies. Hence the high intensity neutrino flux must be peaked in this energy range. Coverage of the sub GeV energy range is desirable to potentially map out the second maximum in the oscillation probability. It is this key physics which dictates the neutrino energy range and thereby the energy range of charged particles which result from neutrino interactions in the ELBNF detectors.

1.2 Single-phase LAr detector

The basic components of the liquid argon detector include a cryostat and associated cryogenic system. A time projection chamber (TPC) and readout electronics are housed in the cryostat.

The cryostat contains the liquid argon target material and the cryogenic system keeps the liquid argon at a cryogenic temperature of 89K, and maintains the required purity through pump and filter system. A uniform electric field is created within the TPC volume between cathode planes and anode wire planes. Charged particles passing through the TPC release ionization electrons that drift to the anode wires. The bias voltage is set on the anode plane wires so that ionization electrons drift between the first several (induction) planes and is collected on the last (collection) plane. Readout electronics amplify and continuously digitize the induced waveforms on the sensing wires at several MHz, and transmit these data to the DAQ system for analysis. The wire planes are oriented at different angles allowing a 3D reconstruction of the particle trajectories. In addition to these basic components, a photon detection system is also included in the design to enable the study of proton decay and be sensitive to galactic supernova neutrinos.

The LAr detector design is characterized by a modular approach in which the LAr volume in the cryostat is instrumented with a number of identical anode wire plane assemblies (APA) and associated cathode plane assemblies (CPA). To a large extent, scaling from detector volumes containing from a few to several hundred of such modules should be straightforward with small and predictable risk.

1.3 Goals for the prototype detector and beam test

The physics sensitivity of ELBNF has been estimated based on detector performance characteristics published in the literature, simulation based estimates as well as a variety of assumptions about the anticipated performance of the future detector and event reconstruction and particle identification algorithms. The proposed single phase LAr prototype detector and CERN beam test aim to replace these assumptions with measurements for the full scale ELBNF detector components and the presently available algorithms. Thereby the measurements will allow to enhance the accuracy and reliability of the ELBNF physics sensitivity projections. The beam measurements will serve as a calibration data set to tune the Monte Carlo simulations and serve as a reference data set for measurements of the future ELBNF detector. In addition, the measurement program aims to evaluate and benchmark the performance of the detector and its individual components. This will allow to identify potentially problematic components and lead to future improvements and optimizations of the detector design.

In order to make such precise measurements, the detector will need to accurately identify and measure the energy of the particles produced in the neutrino interaction with Argon which will range from hundreds of MeV to several GeV. To mitigate the risks associated with extrapolating small scale versions of the single-phase LAr TPC technology to a full-scale detector element, it is essential to benchmark the operation of a full-scale detector elements in a well characterized charged particle beam.

More specifically, the goals of the prototype detector and beam test measurements include the the use of a charged particle beam to:

1. measure the detector calorimetric response for
    (a) hadronic showers
    (b) electromagnetic showers
2. study e/γ-separation capabilities
3. measure event reconstruction efficiencies as function of energy and particle type based on experimental data
4. measure performance of particle identification algorithms as function of energy and for realistic detector conditions
5. assess single particle track calibration and reconstruction
6. validate accuracy of Monte Carlo simulations for relevant energy ranges as well as directions
7. study other topics with the collected data sets
    (a) pion interaction kinematics and cross sections
    (b) kaon interaction cross section to characterize proton decay backgrounds ...
    (c) muon capture for charge identification

For the detector performance characterization a well defined charged particle test beam will enable the following detector performance measurements:

1. characterize performance of full scale TPC module
2. verify functionality of cold TPC electronics under LAr cryogenic conditions
3. perform full-scale structural test under LAr cryogenic conditions
4. study performance of the photon detection system
5. verify argon contamination levels and associated mitigation procedures
6. develop and test installation procedures for full-scale detector components
7. test and evaluate the performance of detector calibration tools

The CERN charged particle beam lines provide an opportunity to perform this crucial test of the proposed single-phase LAr TPC and thereby inform the decision regarding the far detector design and layout for ELBNF. In order to be of greatest value to this decision making process results should be available as soon as possible.

This technical document describes the motivation and technical details for an initial measurement program that we propose to be executed by mid 2018, that is *before* the anticipated LHC long shutdown. The estimated required beam time amounts to $\sim$ XX weeks of data collection. Additional follow-up measurements with potentially modified detector components form a potential extension to the proposed program.

2 Scientific Motivation and Measurement Program [$\sim$10 pages; Donna/Jarek]

The main goal of the Single-Phase Prototype test beam program is to perform measurements that are needed to control and understand systematic uncertainties in DUNE oscillation measurements. The program also includes measurements to support other important DUNE physics measurements as described below.

Work to evaluate effect of all systematic uncertaintes in DUNE sensitivities is still in progress. Current assumptions on detector related systematic uncertainties in DUNE to achieve projected sensitivities [**?**] are shown in Table 1. These are compared with teh levels achieved in MINOS and T2K appearance measurements.

Table 1: Current estimated detector related sources of uncertainty for oscillation measurements.

Source of uncertainty	**MINOS**	**T2K**	**DUNE**	**Comments**
ν_e energy scale	2.7%	2.5%	2%	comment

As an example of the importance of controlling detector related uncertainties, Fig. 2 from Ref. [**?**] shows the effect of various levels of neutrino energy on sensitivities. The nominal sensitivity assumes a 230-kt-MW-year exposure with equal neutrino and antineutrino mode running.

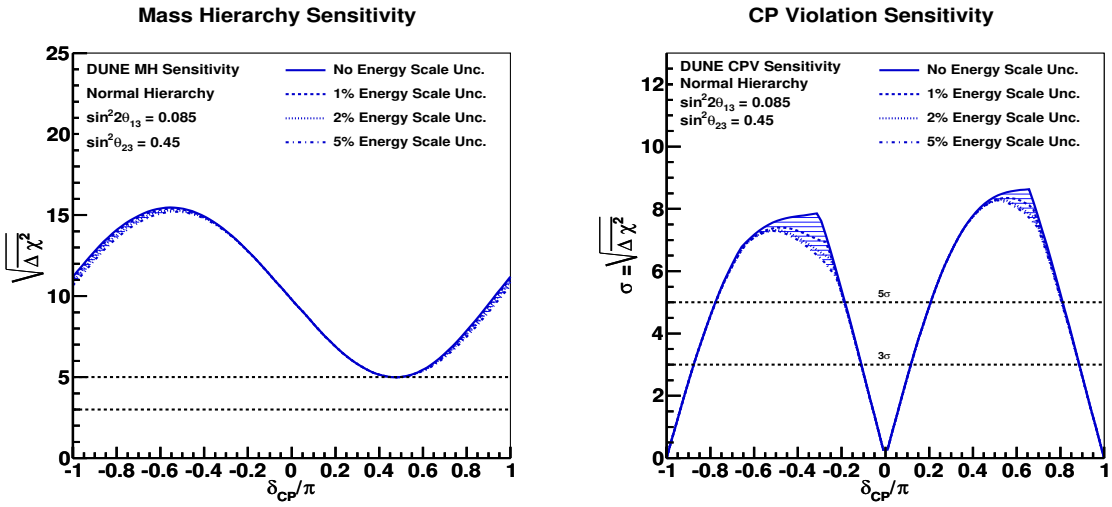

Figure 1: DUNE projected sensitivity dependence of mass hierarchy (left) and δ_{CP} (right) to neutrino energy scale uncertainties. Assumptions are described in the text. If energy scale uncertainties can be controlled at the appropriate levels, DUNE can achieve at least 5σ sensitivity on mass hierarchy determination for 100% of δ_{CP} values and for 3σ sensitivity to δ_{CP} for 75% coverage of phase space.

2.1 Summary of Detector and Beam Requirements

LAr TPC technology was first proposed for use in neutrino experiments by C. Rubbia in 1977 [**?**] but extensive use in neutrino experiments is only now being realized. The ICARUS T600 detector [**?**] pioneered the first large-scale detector operating in the CNGS neutrino beam at mean energy ∼17 GeV. ArgoNEUT [**?**] recently studied neutrino interactions in the NuMI beam down to sub-GeV energies with a small-scale (??-ton) detector. While these samples are proving useful, they do now allow fully isolating the low energy neutrino interaction processes and final states from reconstruction and detector effects. The use of this technology in future precision neutrino experiments will require dedicated information on particle response in the few-GeV to sub-GeV range provided charged-particle test beams.

The DUNE experiment will run beam in both neutrino and anti-neutrino configurations. These beams will be composed mainly of muon neutrinos (anti-neutrinos) as well as electron neutrinos (anti-neutrinos). In Fig. 2.1 the distributions of momenta and angles of particles created in neutrino interactions from simulated beam fluxes are shown.

The detector is designed to mimic the current DUNE Far detector design but must be sufficiently large in both longitudinal and transverse dimensions to contain showering particles up to the energy range of interest (∼7 GeV). Fig. 2.1 shows the simulated longitudinal and transverse containment for proton showers up to 10 GeV/c momentum. For 10 GeV showers, more than 95% of the energy is contained in a detector of longitudinal size of 550 cm and radius of 200 cm. Shower from pions, kaons, and electrons have also been studied and better containment is achieved in those cases.

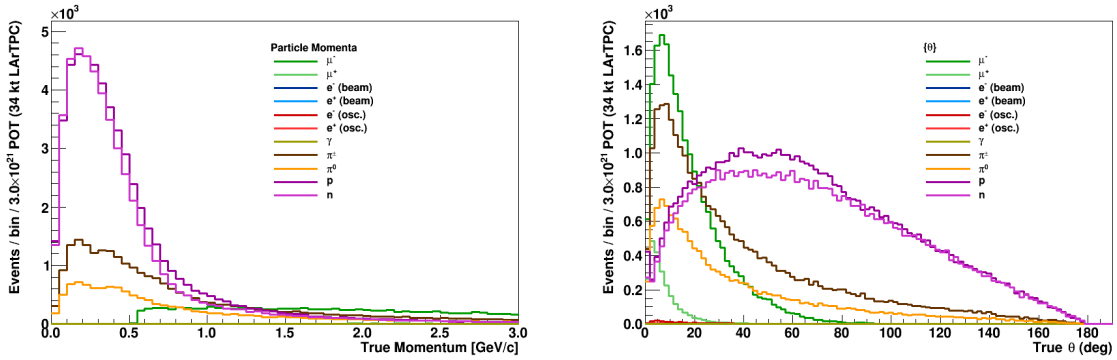

Figure 2: Particle momenta (left) and angular (right) distributions for particles produced in neutrino interactions from ν_e, ν_μ, $\bar{\nu}_e$ and $\bar{\nu}_\mu$ at the far detector location.

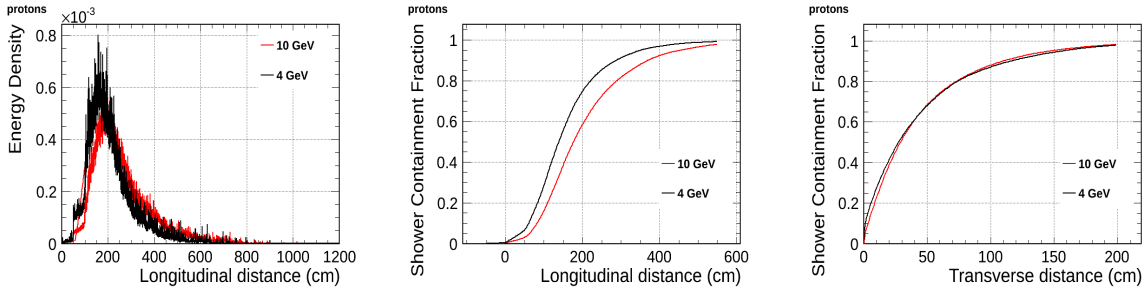

Figure 3: Simulated longitudinal and transverse containment for proton showers of 4 and 10 GeV/c momenta.

2.1.1 Summary of Beam Particle Requirements

Table 2 summarizes the requested particle types and momenta along with required exposures for the test beam program.

2.2 Detector performance tests

2.2.1 Bethe-Bloch parametrisation of charged particles

The prototype detector will allow to study the detector response to charge particles from the test beam and will serve as a calibration detector. The measured energy deposition for various particles and its dependence on the direction of the particle will feed into our Monte Carlo generator and allow more precise reconstruction of neutrino energy and interactions topologies with good particle identifications.

How we compare with Lariat? Multiple scattering

The set of single-phase prototype detector helped to understand the detector response to cosmic muons. But there is still lots to learn with additional studies. The charge particle identification efficiencies has been mapped for only limited range of the particle energies.

Particle	Momenta (GeV/c)	Exposure	Purpose
π^+	0.2, 0.3, 0.4, 0.5, 0.7, 1, 2, 3, 5, 7	10K	hadronic cal, π^0 content
π^-	0.2, 0.3, 0.4, 0.5, 0.7, 1	10K	hadronic cal, π^0 content
π^+	2	600K	π^o/γ sample
e^+ or e^-	0.2, 0.3, 0.4, 0.5, 1, 2, 3, 5, 7	10K	e-γ separation/EM shower
μ^-	(0.2), 0.5, 1, 2	10K	E_μ, Michel el., charge sign
μ^+	(0.2), 0.5, 1, 2	10K	E_μ, Michel el.,charge sign
μ^- or μ^+	3, 5, 7	5K	E_μ MCS
proton	0.7, 1, 2, 3	10K	response, PID
proton	1	1M	mis-ID pdk, recombination
antiproton	low-energy tune	(100)	antiproton stars
K^+	1	(13K)	response, PID, PDK
K^+	0.5, 0.7	(5K)	response, PID, PDK
μ, e, proton	1 (vary angle $\times 5$	10K	reconstruction

Table 2: Requirements summary for particle types and momenta. Items in parenthesis indicate lower priority (see text).

2.2.2 e/γ separation

The search for a CP violation phase using ν_e appearance in a ν_μ beam requires good electron/photon separation. Backgrounds originating from photons produced primarily from final state π^0's must be identified and removed from the signal electron sample.

The photons can undergo two process: pair production and Compton scattering. The dominant process for photons with energies of several hundreds MeV is the e^+ e^- pair production, but Compton scattering also occur at this energies. For pair production the e/γ separation is achieved by looking at the beginning of the electromagnetic shower, where for election we see energy deposition typical for single MIP and for photon we see energy deposition consisted with two MIPs. In case of Compton scattering off of atomic electrons the signal is much more difficult to distinguish from the CC ν_e scattering signal.

Electron-photon separation has been studied in LAr TPCs (Icarus and Argoneut) as shown in Fig. **??**. Currently the separation efficiency is estimated to be at the level of of 94 % (? cite and check the number). This may depend on particular features of the geometry including wire pitch, etc. Therefore, it is critically important to study e/γ separation in a prototype LAr TPC detector. **we need someone to look into this**

2.2.3 Reconstruction efficiencies and particle identification

The reconstruction of events in the LAr TPC is still a challenge but rapid progress has been achieved in recent years (cite pandora and other reconstruction algorithms). Despite the progress reconstruction algorithms have to rely Monte Carlo predictions which don't simulate liquid argon detectors responses correctly. Reconstruction algorithms will benefit greatly from test beam data particularly from the full scale prototype. The reconstruction algorithms will be trained to correctly reconstruct track, electromagnetic and hadronic showers. The data of tracks and showers can be used to create a library of reference events with which to tune algorithms.

Main issues for the reconstruction algorithms:

- The reconstruction algorithms try to use all three planes on the signal readout. if the orientation of the track/shower is such that it is aligned with wires on one of the plans it significantly reduces quality of reconstructed objects.
- Calorimetry with collection and induction planes. In the ICARUS experiment the deposited energy was reconstructed from the signal on the collection plane. The induction planes bipolar signal wasn't "stable" enough to use it for calorimetric measurement. In the ELBNF design there is additional shielding wire plane which will improve the quality of the bipolar signal and the test beam experiment will help with its calibration.
- Vertexing.
- Reconstruction efficiency for low energy particles. The reconstruction algorithm suffer from the lose of efficiency for low energy particle or particles which leave less than 200-300 hits. Training the algorithms on a low energy particles from the test beam will improve the quality and efficiency of the reconstructed objects.

2.2.4 Cross section measurements

Precise measurement of the absorption and charge exchange of pions and kaons. Pion absorption is a large part of the pion nucleon cross section from 50 MeV to 500MeV with no data above about 1GeV pion kinetic energy. **Add plots and values for known cross sections wit errors**

- pion absorption on argon - Kotlinski, EPJ 9, 537 (2000)
- pion cross section as a function of A - Gianelli PRC 61, 054615 (2000)

There is not currently a satisfactory theory describing absorption. The Valencia group (Vicente-Vacus NPA 568, 855 (1994)) developed model of the pion-nucleus reaction with fairly good agreement, although not in detail. The actual mechanism of multi-nucleon absorption is not well understood.

2.2.5 Charge sign determination

It is not possible to determine charge of the particle on the event by event basis with non-magnetised LAr TPC detectors. A statistical separation will be studied which will make use of differences in muon versus antimuon capture cross sections and lifetime. For the μ^+ for argon we expect about xx% to be captured and for μ^- about yy%.

2.2.6 Single track calibration

2.2.7 Shower calibration

Reconstruction of neutrino energy depends of a quality of reconstruction of both electromagnetic and hadronic showers.

- **features of Hadronic shower in LAr TPC - features of electromagnetic shower in LAr TPC** - Missing energy from neutral (Neutrons scattering)

2.3 Other measurements

2.3.1 Anti-proton annihilation

A sample of antiproton would be useful to calibrate the p-$\overline{p}$ annihilation process. This would provide input to exotic B-violating process neutron oscillation (reference) modeling of subsequent n-$\overline{n}$ annihilation. These events would be taggged in the mixed-mode beam. Events should be at the lowest energies achievable in this beamline.

2.3.2 Proton decay sensitivity and background samples

The DUNE experiment in the deep underground location will improve sensitivity to detection of several modes of proton decay. In particular, a first ever LAr detector of this scale underground will primarily improve sensitivity to proton decays with final state kaons such as $p \to K^+\overline{\nu}$. Sensitivity to this process is studied in [**?**]. K^+ detector efficiencies are estimated to be >97% in the appropiate momentum range (500-800 MeV/c). The kaon samples requested in Table 3 are needed to directly measure K^+ PID and detection efficiencies. Obtaining low energy kaons will likely be difficult in this beamline. A sample of 13K beam kaons with 1 GeV/c momentum are requested to provide 2K stopping K^+ track samples for PID studies. (only 15% of K^+ at 1 GeV stop at 1 GeV/c).

Particle	Momenta (GeV/c)	Exposure/bin
K^+	1	(13k)
K^+	0.5, 0.7	(5k)
proton	1	(1M)

Table 3: Samples related to proton decay physics requirements.

A sizable sample of protons ($\sim 10^6$) are requested to study the possible background contributions to $p \to K^+\overline{\nu}$. This sample of protons are needed to quantify the possibility that an interacting **p** is *mis-IDed as stopping K*. A proton interaction which produces neutrals and one charged pion (which is mis-IDed or subsequently decays to μ) can fake the final state kaon signal.

2.3.3 Supernova

The energies of the electrons coming from CC ν_e interactions from Supernova will be in the order of 10s of MeV. The beam test cannot offer such low energy electron, but one can use the Michel electrons form $'mu$ decay to cover these energies. The SK used the Michel spectrum to calibrate the absolute energy scale.

3 Single Phase LAr Detector [~10 pages; J. Stewart et al.]

3.1 ELBNF detector

The far detector for the DUNE collaboration will be a series of four liquid argon time projection chambers (TPC), each in a cryostat that holds a fiducial/active/total LAr mass of 10.0/13.3/16.9 kt. The TPCs will be instrumented with photon detection. It is planned that the first 10 kt detector will be ready for installation in the 2021 timeframe. One option for the TPC design is a wire plane based TPC with cold electronics readout. Designs of this style are are referred to as single-phase detectors as the charge generation, drift, and detection all occurs in the argon liquid phase. This style TPC has the advantage that there is no charge amplification before collection making a very precise charge measurement possible. To achieve DUNE's goals, a detector much larger than ICARUS, the largest LAr TPC detector built to date, is needed. The LBNE experiment was developing a scalable far detector design shown in Figure 4 that would scale-up LAr TPC technology by roughly a factor of 40 compared to the ICARUS T600 detector. To achieve this scale-up, a number of novel design elements need to be employed. A membrane cryostat typical for the liquefied natural gas industry will be used instead of a conventional evacuated cryostat. The wire planes or anode plane assemblies (APAs) will be factory-built as planar modules that are then installed into the cryostat. The modular nature of the APAs allow the size of the detector to be scaled up to at least 40 kt fiducial mass. Both the analog and digital electronics will be mounted on the wire planes inside the cryostat in order to reduce the electronic noise, to avoid transporting analog signals large distances, and to reduce the number of cables that penetrate the cryostat. The scintillation photon detectors will employ light collection paddles to reduce the required photo-cathode area. Many of the aspects of the design will be tested in a small scale prototype at Fermilab but given the very large scale of the detector elements a full-scale test is highly desirable. As the new DUNE collaboration forms and organized a combined detector design team will emerge. Ideas from this new collaboration will modify the design presented here but this design provides a concrete example of a possible future detector.

The goals of the DUNE detector test can be broken into four categories: argon contamination mitigation verification, TPC mechanical verification, TPC electrical verification, and photon detection light yield verification. Research at Fermilab utilizing the Materials Test Stand has shown that electronegative contamination to the ultra-pure argon from all materials tested is negligible if the material is under the liquid argon. This implies that the dominant source of contamination originates from the gas ullage region and in the room temperature connections to the detector. Careful design of the ullage region to insure that all surfaces and feedthroughs are cold is expected to greatly reduce the sources of contamination over what exists in present detectors. Other concepts attempt to eliminate the gas ullage completely. The goals related to mechanical testing are to test the integrity of the detector. In the current design, each APA measures 2.3 m by 6.0 m and includes 2560 wires and associated readout channels. Given the complexity of these assemblies, a test where the detector can be thermally cycled and tested under operating conditions is highly advised prior to mass production. The

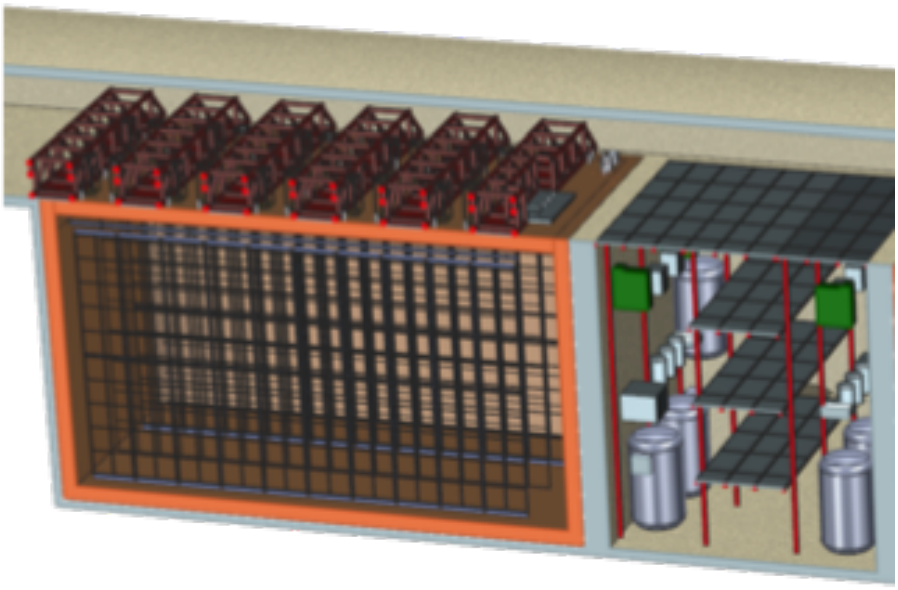

Figure 4: 3D model of one design of the DUNE single-phase detector. Shown is 5kt fiducial volume detector which would need to be lengthened for the 10 kt design. The present DUNE plan calls for the construction of 4 10 kt detectors of similar design.

mechanical support of the APAs can be tested to verify that the mechanical design is reliable and will accommodate any necessary motion between the large wire planes. The impact of vibration isolation between the cryostat roof and the detector can also be tested. Finally a potential improvement in the cryostat design is the possibility to move the pumps external to the main cryostat. This will reduce any mechanical coupling to the detector and also greatly improve both reliability and ease of repair. The electrical testing goals are to insure that the high voltage design is robust and that the required low electronic noise level can be achieved. As the detector scale increases so does the capacitance and the stored energy in the device. The design of the field cage and high voltage cathode planes needs to be such that HV discharge is unlikely and that if the event occurs no damage to the detector or cryostat results. The grounding and shielding of large detectors is also critical for low noise operation. By testing the full scale elements one insures that the grounding plan is fully developed and effective. Large scale tests of the resulting design will verify the electrical model of the detector.

3.2 CERN prototype detector

3.2.1 Overview of the CERN Single-Phase test Detector

This sections presents the design details of a single-phase detector based on the development of the LBNE collaboration. As DUNE moves forward, the TPC working group will evaluate this and any modifications or alternate proposals. For the purpose of this proposal this represents one alternate, and it is expected to evolve as the new collaboration is organized and more work is done.

This TPC consists of alternating anode plane assemblies (APAs) and cathode plane

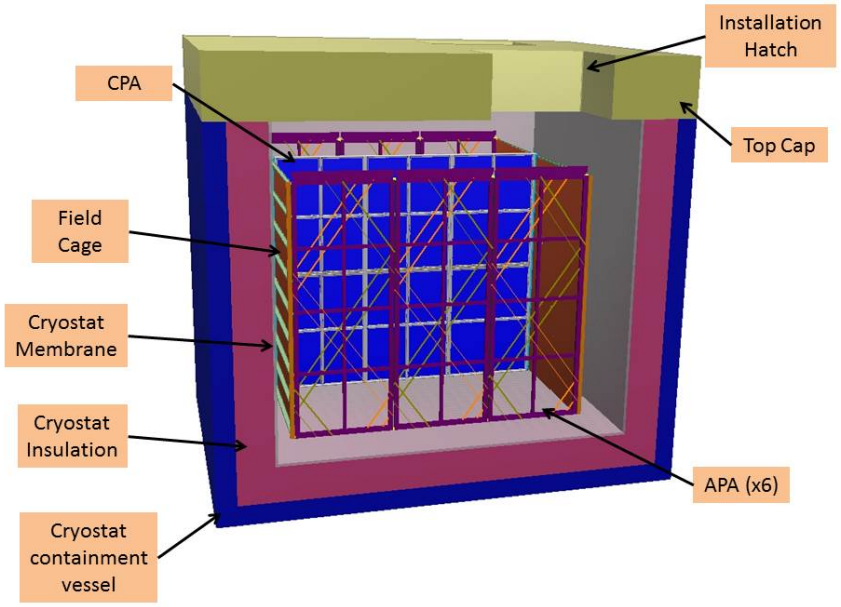

Figure 5: 3D model of the single-phase detector prototype is shown inside the test cryostat.

assemblies (CPAs), with field-cage panels enclosing the four open sides between the anode and cathode planes. Figure 5 shows a sectioned view for the planned TPC inside the cryostat at CERN. A uniform electric field is created in the volume between the anode and cathode planes. A charged particle traversing this volume leaves a trail of ionization. The electrons drift toward the anode plane, which is constructed from multiple layers of sense wires, inducing electric current signals in the front-end electronic circuits connected to the wires.

To the extent possible the TPC will be assembled from elements that are of the same size as those planned for the single phase far detector. The primary exception to this is the length of the field cage panels which are 2.5m in this design, compared to 3.6m in the far detector. This is because the drift distance between the APA and CPA is reduced to lessen the impact of space charge on the prototype necessitated by the surface operation. We are currently considering a test that will initially have a drift distance of 3.6m to prove the mechanics of the far detector design. The cryostat will then be emptied and the planes shifted to the surface design of 2.5m. The overall size of the TPC will be derived by the size and number of anode planes (APA). It has been determined in order to perform the required physics, the TPC will have a 3-APA wide active volume. The APAs will have an active (total) area 2.29 m (2.32 m) wide and 6.0 m (6.2 m) high. The combination of the three APAs determines the overall TPC length to be 7.3m. There will be a cathode plane (CPA) in the center between the two rows of APAs. The overall width of the TPC will be determined by a combination of the drift distances along with the thickness of the APA, which is constructed of 76.2 x 101.6 mm stainless steel (SS) structural tubing. The overall width of the TPC is 7.4m. Like the length of the TPC, the overall height will be determined by the height of the APA which is 6.4m. In summary the external TPC dimensions will be 7.3m long x 7.4m wide

x 6.4m high. Along with the APAs and CPAs, the TPC will include a field cage that surrounds the entire assembly. This is a series of pultruded fiberglass I-beams for the structural elements. These I-beams will be tiled with large copper sided FR4 panels to create the field cage. Each panel will be connected with a series of resistors. The field cage will be connected to the CPAs through a capacitor assembly.

All of this will be supported by rows of I-beams supported from a mechanical structure above the cryostat. The hangers for these I-beams will pass through the insulated top cap. There will be a series of feed thru flanges in the top cap of the cryostat to bring in and take out services for the TPC. There will be a HV feed thru for each of the CPA rows and one signal feed thru for each of the APAs.

The minimum internal size of the cryostat is 8.9m long, 7.8m wide and 8.1m high. This is determined by adding the necessary mechanical and electrical clearances to the computed size of the TPC. The current plan is to have the CPA located in the center of the cryostat with a APAs on each side near the walls of the cryostat membrane. The above dimensions preserve the ability to reverse the order of the TPC rows by placing the CPAs next to the walls of the cryostat and the APAs in the center. However, this can only be done with the shorter 2.5m drift distance. This reversed configuration, at the 3.6m drift planned for the far detector, will place the CPAs too close to the membrane to avoid high voltage discharge and possible damage of the membrane.

3.2.2 Anode Plane Assemblies (APAs)

Each APA (Figure 6) is instrumented with 3 layers of signal wires, one longitudinal collection plane and two 35.7° angled induction planes with an additional outer grid plane that helps maintain the field. The overall dimensions of the active area as mentioned able are 2.3 m wide, 6 m long. The dimension of the wire planes were selected to fit down the Ross shaft at SURF, be compatible with a standard HiCube transport container, and allow construction from readily available materials. The angled layers start at the electronics end and wind around to the other side on their way to the bottom. The wire angle was selected so that a given angled induction wire will not overlay any longitudinal collection wire more than once in order to reduce ambiguities caused by the wrapped wire construction. Partial wire layers are shown here in Figure 6 at the bottom. With a wire pitches of 4.67 mm (diagonal layers) and 4.79 (straight layers), the total number of readout channels in an APA is 2560. The grid layer is not depicted in Figure 6 for clarity. The underlying structure of each APA is a framework of rectangular, stainless steel tubing. The side and bottom edges of the frame are lined with multiple layers of fiberglass circuit boards, notched along the edges to support and locate the wires that cross the APA face. A set of FR4 combs are glued to the APA frame to capture the wires at regular intervals. The front-end electronics boards are mounted at the top end of the frame and protected by a metal enclosure.

The distance between wire planes is 4.8 mm (3/16 in) corresponding with standard printed circuit board thickness, and while maintaining optimal signal formation. The four wire planes will be electrically biased so that electrons from an ionizing-particle track completely drift past the first three planes and are collected by the fourth plane. Calculations show that the minimum bias voltages needed to achieve this goal are V_G = -665V, V_U = -370V, V_V = 0V and V_X = 820V respectively (where G, U, V, and X

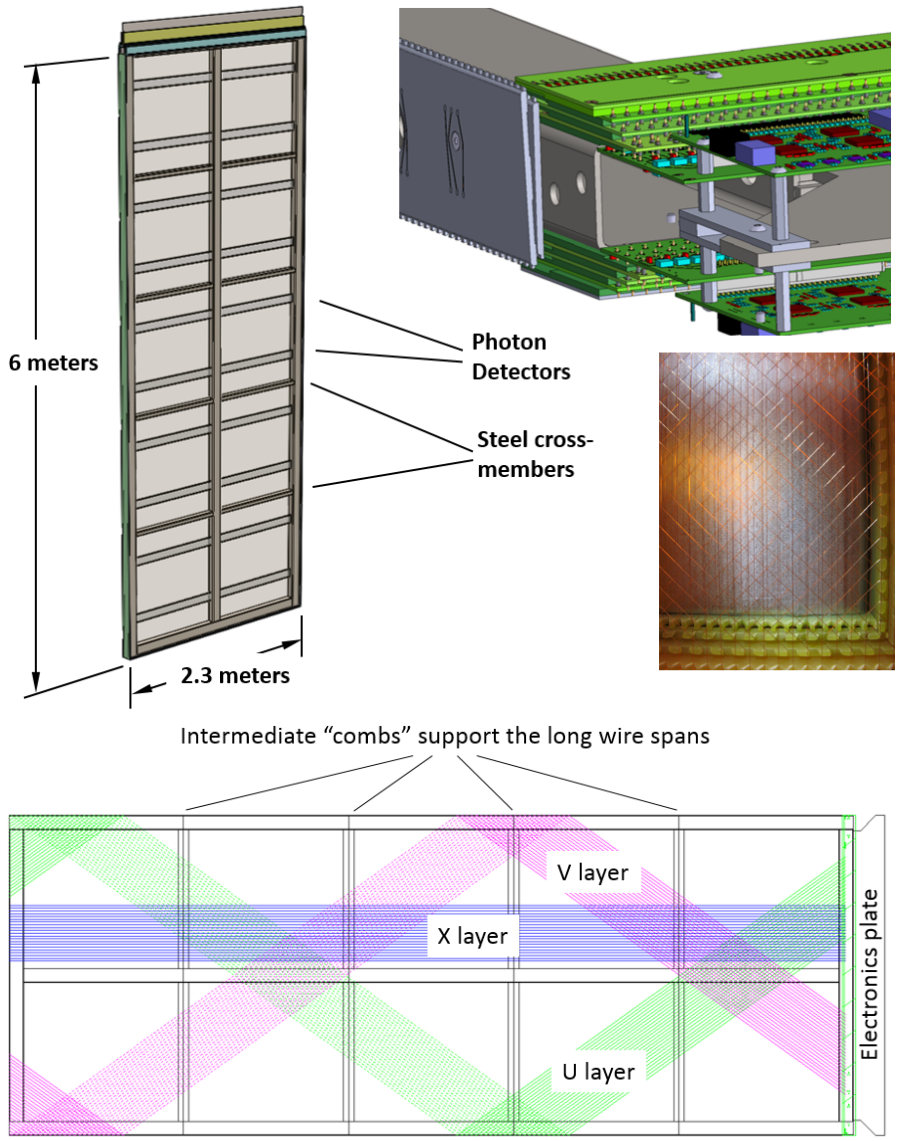

Figure 6: Clockwise from left: A full size APA, an APA corner showing the electronics boards, an APA lower corner photo showing wires and edge boards, and a figure showing the wire orientations and the placement of wire aligning combs.

are the wire-layer labels from outside in, towards the frame). It is convenient to set one of the wire planes to ground so that the wires can be DC coupled to the front-end readout electronics. In this instance, the V wire plane is set to ground potential to reduce the maximum bias voltages on the other wire planes, and enable the use of lower voltage rated AC coupling capacitors. A grounded mesh plane, located 4.8 mm behind the collection (X) plane, prevents the electric field around this set of wires from being distorted by the metal frame structure and the wires on the opposite side of the frame. It also shields the sensing wires from potential EM interferences from the photon detectors (Fig. 3.2.2) mounted within the frame. The mesh should have a wire pitch less than 2 mm to ensure a uniform electric field while maintaining a high optical transparency.

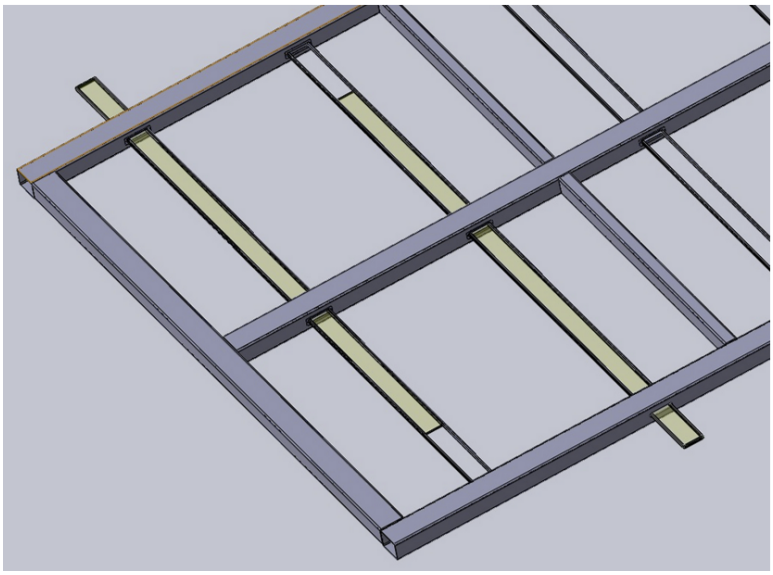

Figure 7: Photon detectors are mounted within the frame, between the wires on the two sets of four wire layers. The APA is built so that the photon detectors can be installed through slots in the side of the APA after the APA wires are installed. The wires that would cross these slots are routed around using copper traces on the edge boards.

3.2.3 CPA and Field Cage

Each cathode plane (Fig. 8) is constructed from 6 identical CPA (cathode plane assembly) modules and two sets of end pieces. Each CPA is about half the size of an APA (2.3m $\times$ 3.1m) for ease of assembly and transport. The CPA is made of a stainless-steel framework, with 4 pieces of thin FR4 sheets mounted in the openings. A receptacle for the HV feedthrough is attached to the upper corner of a cathode plane toward the roof entrance side to mate with the HV feedthrough in the cryostat ceiling.

The FR4 sheets on the CPAs are treated with layers of high resistive coating on both sides. The resistivity of the coating will be chosen such that the surface potential does not deviate significantly with the ionization current from the cosmic rays, and forms a relatively long time constant to dissipate the stored energy on each sheet in case of a high voltage discharge. This long RC time constant will also reduce the peak current injected into the front-end electronics in a HV discharge.

Due to the relatively high cosmic ray flux in this surface detector, it is preferable to prevent the scintillation light emitted by a cosmic ray between the cathode and cryostat wall from entering the TPC to reduce false trigger. The opaque cathode surface will service this purpose. The high flux of cosmic rays combined with very low drift velocity of positive ions in the liquid argon will result in sizable space charge distortions in the TPC (docdb #6471). In addition, the positive ions could build up further if the ion motion is slowed or stalled by counter flow in the LAr. Preliminary CFD analysis (docdb #6140) have shown that solid cathodes in the cryostat result in LAr flow pattern that neither causes excess positive ion buildup, nor degrades the LAr purity.

To achieve a 500 V/cm drift field over a 2.5 m distance, the bias voltage on the cathode plane must reach -125 kV. Two high voltage power supplies (150 – 200 kV) and

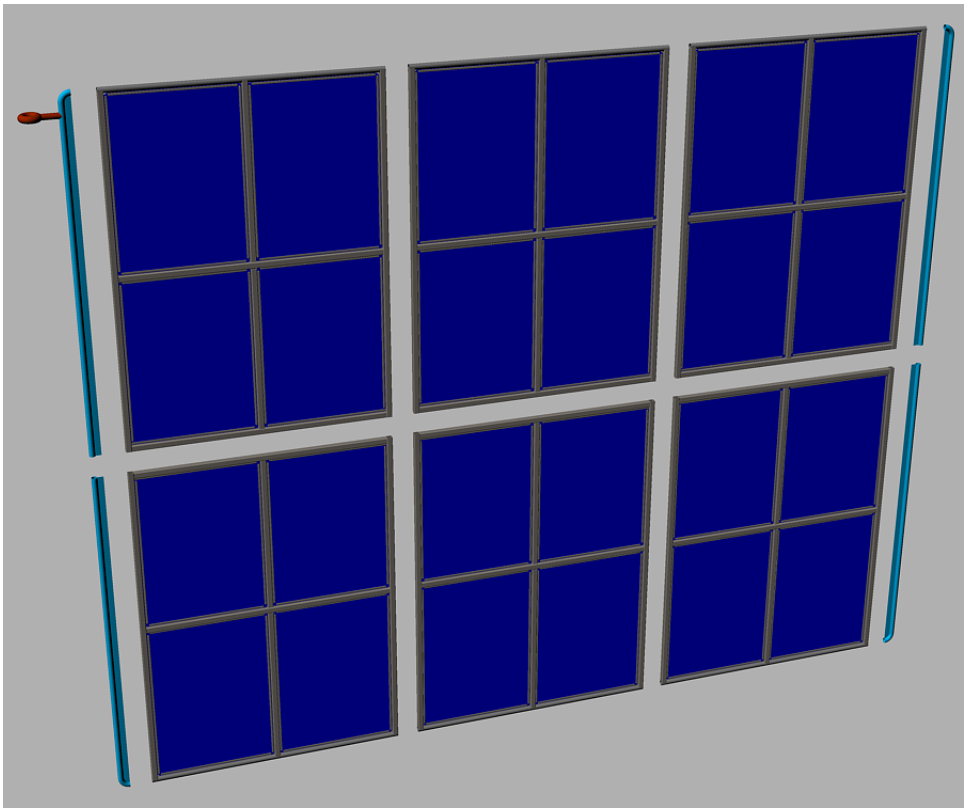

Figure 8: Exploded view of a cathode plane constructed from 6 CPA modules and 4 end pieces. The facing material on the CPA is highly resistive to minimize the peak energy transfer in case of a HV breakdown.

two HV feedthroughs will be needed for the two cathode planes. The HV feedthroughs are based on the Icarus design, but modified to further improve the stability at higher voltages.

Each pair of facing cathode and anode rows forms an electron-drift region. A field cage completely surrounds the four open sides of this region to provide the necessary boundary conditions to ensure a uniform electric field within, unaffected by the presence of the cryostat walls.

The field cages are constructed using copper-clad FR4 sheets reinforced with fiber glass I-beams to form panels of 2.5 m $\times$ 2.3 m in size for the top and bottom modules, and 2.5 m $\times$ 2 m modules for the sides. Parallel copper strips are etched or machined on the FR4 sheets. Strips are biased at appropriate voltages through a resistive divider network. These strips will create a linear electric-potential gradient in the LAr, ensuring a uniform drift field in the TPC's active volume.

Since the field cage completely encloses the TPC drift region on four (of six) sides, with the remaining two sides blocked by the solid cathodes, the FR4 sheets must be frequently perforated to allow natural convection of the liquid argon. The "transparency" of the perforation will be determined by a detailed LAr computerized fluid dynamic (CFD) study.

The left of Figure 9 shows a section of the field cage in the 35ton TPC as it was being assembled. The 35ton TPC test results will inform us whether we should improve

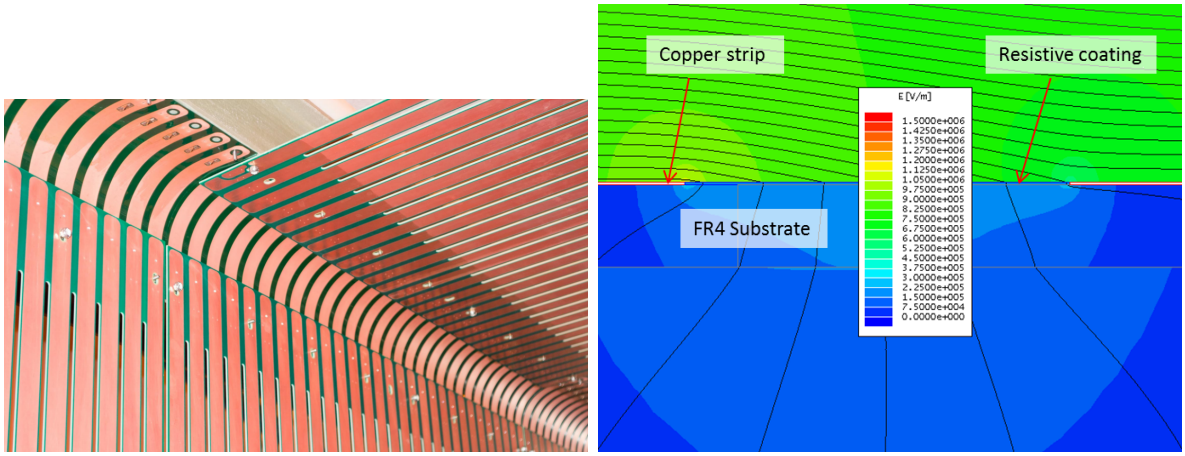

Figure 9: Left: A section of the field cage in the 35ton TPC. Right: Plot of electric field (color contours(and equi-potential contours (black lines) in a small region around the edges of two adjacent field cage strips on a 1.6mm thick FR4 substrate. A layer of resistive coating between the two copper strips nearly eliminated the high electric field regions at the copper edges

upon the current design, or change the design concept all together for this and future detectors. The main concern with the current field cage design is that the electric field at the edges of the copper strips is still quite high due to the thinness of the copper. One possible remedy is to cover the entire surface of the field cage with a high resistive coating. The resistivity between strips due to this coating must be kept many orders of magnitudes higher than the divider resistance to avoid distortion to the drift field. Figure 9 (Right-Panel) shows an FEA simulation of such a configuration.

In the event of HV discharge on the cathode or the field cage, the voltage differential between neighboring field cage strips near the discharge electrode will be very high for a brief moment. This over voltage condition could cause damage to the field cage electrode and the resistors installed between strips. To minimize such disk, varistors or gas discharge tubes (GDT) will be installed between the field cage strips in parallel with the resistors to prevent excess voltage transient between the electrodes.

In order to test the installation concept of the far detector, the top and bottom field cage modules will be attached to the mating CPAs through hinges. These combined assembly will be installed into the cryostat and the field cage module opens to bridge the CPA and the APA both mechanically and electrically.

3.2.4 TPC Readout

The TPC electronics is designed to operate at liquid argon temperature and is placed as close to the sense wires as possible, thus minimizing the capacitance and the preamplifier noise. The present design has a maximum wire length of 7.3 m (induction planes) with a corresponding capacitance of 164 pF and an expected intrinsic noise of 400 electrons. The preamplifiers include shaping circuits, and are implemented in 16 channel front-end (FE) ASICs, which couple directly to 16 channel, 12 bit ADC ASICs operating at 2 MS/s, which include a 1:8 multiplexing stage. The ADCs are read out by a commercial FPGA,

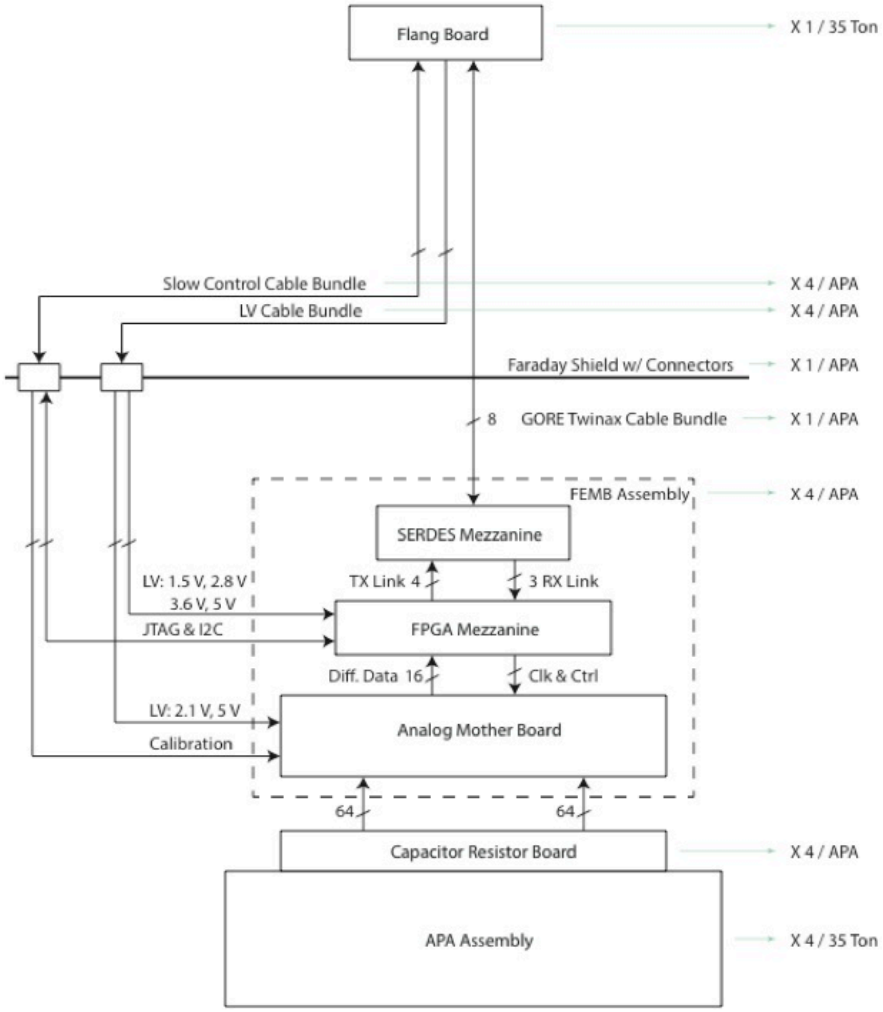

Figure 10: Layout of the TPC cold from end (FE) electronics..

which provide an additional factor of 4 in multiplexing. This level of multiplexing is low enough for transmitting the entire raw data stream, while also being high enough that the number of signal lines is actually smaller than the number of the various power and control lines, and therefore easily manageble by a small number of feedthroughs. Neither zero suppression nor data compression is implemented at the level of the cold readout electronics. Not only does this greatly simplify the cold electronics design, but it also automatically satisfies the requirement that the system be capable of such raw readout, and further eliminates an entire class of failure-modes. The FPGAs transmit the data via high-speed (1 Gbps) serial links to the DAQ system. For the final detector it is expected that a dedicated digital control and data transmission ASIC (COLDATA) will be developed which replaces the commercial FPGA. While the COLDATA is well under way, it is not expected to be available in time for the CERN test, which will instead make use of the proven FPGA technology. While serious doubts regarding the longevity of commercially-available FPGAs at LAr temperatures strongly argues against their use in the Far Detector, where reliability over 15-20 years is required, this is not a

concern for the CERN test, where the proven FPGA lifetime of at least a year is more than adequate.

The front end electronics is organized as a stack of three boards comprising the Cold Mother Board assembly (CMB), which mounts directly on the APA. First is the Analog Mother Board, on which are mounted the FE and ADC ASICs. Second and third are the FPGA and SERDES Mezzanine Boards, themselves mounted on the Analog Mother Board. Each CMB has eight sets of FE and ADC ASICs and instruments 128 wires. A Faraday cage (FC) covers the end of the APAs to shield the electronics from ambient noise. The FC also serves to prevent any Ar gas-bubbles from LAr boiled by the electronics' heat from entering the active TPC volume. Figure 10 shows a schematic of the cold electronics.

Besides the high-speed signal cable, which is a twin-axial cable bundle manufactured by GORE, there are cable bundles for low-voltage power, wire-bias voltages, and various slow controls and monitoring. The cable bundles will be connected through a feedthrough on the roof of the cryostat.

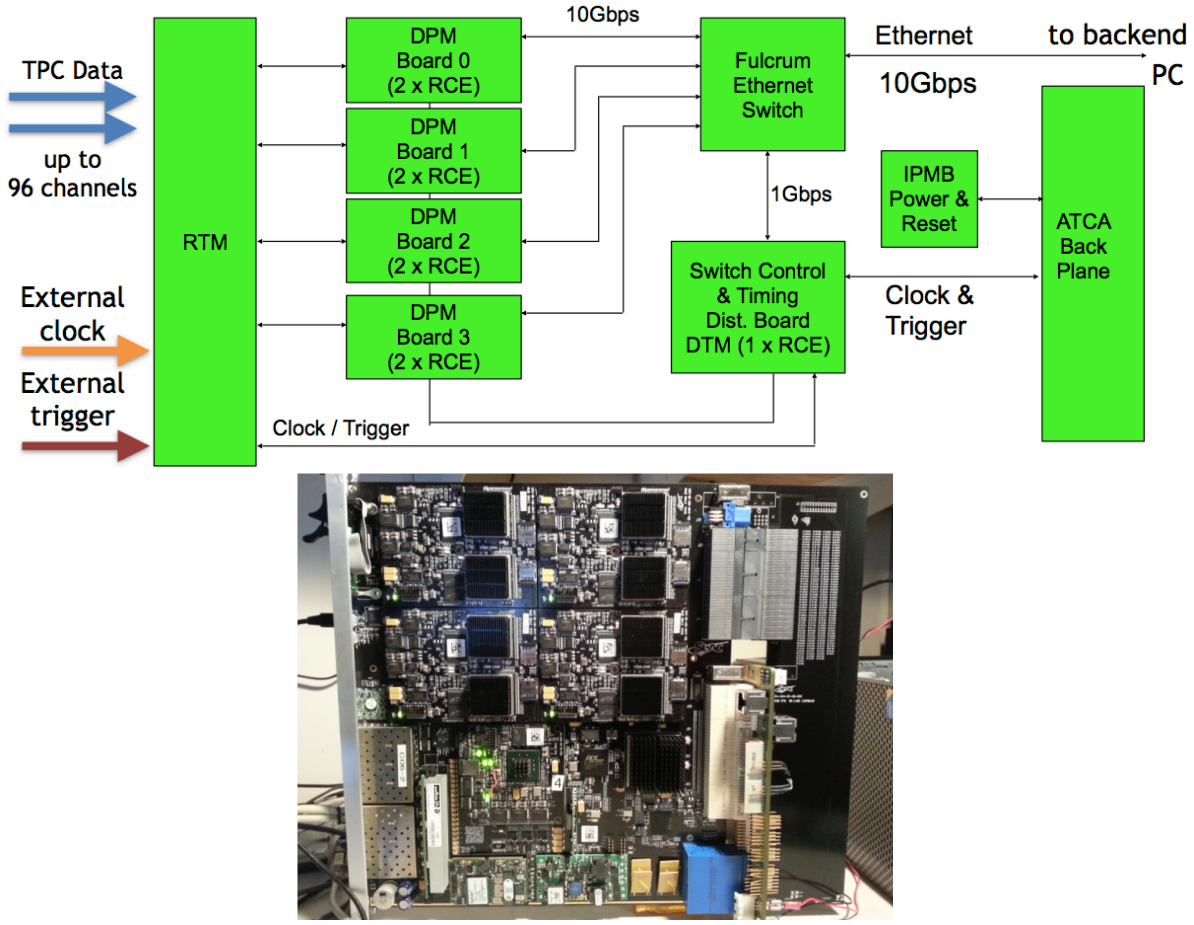

Figure 11: Top: Schematic for the TPC DAQ system. Bottom: The COB (left of the large connectors) and RTM (right).

The primary interface between the TPC front-end electronics (FE) and the DAQ subsystem consists of an ATCA-based system of RCEs (Reconfigurable Cluster Elements).

The RCE system receives the serialized raw data for the FE, performs zero-suppression on it, and packetizes and transmits the resulting sparsified data to a back-end data farm for event building and further processing. Additionally, the RCE system transmits timing and control signals to the FE as well as forwarding configuration data to them at start-up.

The RCE system consists the following components: a commercial ATCA shelf (2-, 6-, or 14-slot), a Cluster-On-Board (COB) which is the "front board" in ATCA terms, and a Rear-Transition-Module (RTM) which is the "rear board". A schematic of the system is shown in Figure 11. The COB is a custom board, developed by SLAC, which holds the processing power of the system. The COB (see Figure 11) consists of 5 bays for holding daughter boards, an onboard 10-GbE switch, and both 10- and 1-Gb ethernet connections for communications with the back-end system. Four of the daughter-board bays are for Data Processing Modules (DPM), each of which can hold up to two RCEs. The RCE is the core procession unit of the system; it is made up of a modern SoC (currently, the Xilinx Zynq-7045) with multiple high-speed I/O ports (up to 10-Gbps each) and external DRAM and flash memory controllers. The other bay on the COB contains the Data Transmission Module (DTM) which is responsible for distributing timing and trigger information to and between the DPMs.

While the COB hardware is application agnostic, the RTM is application specific. The RTM provides the mechanical interface between the front-end (or, in our case, the flange electronics) and the back-end, as well as other external sources such as the timing or trigger systems. In this case we will use fiber optic connections between the flange and the TPC DAQ using 8 12-channel (full duplex) CXP connectors on the RTM.

With the assumption that each cold FE board multiplexes it's 128 wire channels to 4 outputs at 1-Gbps each, the non-zero suppressed data for 1 APA can be fed into a single COB (containing 8 RCEs). Each RCE would receive data from 2 FE boards, perform zero-suppression, and send the result to the back-end.

3.2.5 Photon Detection System

The ELBNF far detector will utilize liquid argon scintillation light to determine the prompt event time of beam-driven and non-beam events. While the TPC will have far superior spatial resolution to a photon detection system, the drift time for TPC events is on the order of milliseconds. The beam clock will give much better timing resolution than this but a photon detection system can determine the start of an event occurring in the TPC volume (or entering the volume) to about 6 ns, which will be useful in determining the t_0 of cosmic ray events, events from radiological decays, and corrections to energy loss of the drifting electrons.

A charged particle passing through liquid argon will produce about 40,000 128 nm photons per MeV of deposited energy. At higher fields this will be reduced due to reduced recombination, but at 500 V/cm the yield is still about 20,000 photons per MeV. Roughly 1/3 of the photons are prompt 2-6 ns and 2/3 are generated with a delay of 1100-1600 ns. LAr is highly transparent to the 128 nm VUV photons with a Rayleigh scattering length and absorption length of 95 cm and >200 cm respectively. The relatively large light yield makes the scintillation process an excellent candidate for determination of t_0 for non-beam related events. Detection of the scintillation light may

also be helpful in background rejection.

Several prototypes of photon detection systems have been developed by the LBNE, now ELBNF, photon detector group over the past few years. There are currently three prototypes under consideration for use in the ELBNF far detector, a baseline design along with two alternate designs. A decision on the design to be deployed in the CERN test will be made in late 2015. The CERN neutrino platform ELBNF test would provide the first full scale test of the ELBNF photon detector fully integrated into a full scale TPC anode plane assembly.

The present reference design for the photon detection system is based on acrylic bars that are 200 cm long and 7.63 cm wide, which are coated with a layer of tetraphenyl-butadiene (TPB). The wavelength shifter converts VUV (128 nm) scintillation photons striking it to 430 nm photons inside the bar, with an efficiency of 50% of converting a VUV to an optical photon. A fraction of the wavelength-shifted optical photons are internally reflected to the bar's end where they are detected by SiPMs whose QE is well matched to the 430 nm wavelength-shifted photons. All PD prototypes are currently using SensL MicroFB-6K-35-SMT 6 mm ? 6 mm devices.

A full 6 m long APA will be divided into 5 bays with 2 PD modules (paddles) instrumenting each bay. The paddles will be inserted into the frames after the TPC wires have been wrapped around the frames allowing final assembly at the CERN test location. Two alternative designs are also under consideration.

One alternate design targeted increasing the geometrical acceptance of the photon detectors by using large acrylic TPB coated plates with imbedded WLS fibers for readout. In this design the number of required SiPMs and readout channels per unit detector area covered with photon detection panels would be significantly reduced to keep the overall cost for the photon detection system at or below the present design while increasing the geometrical acceptance at the same time. The prototype consists of a TPB-coated acrylic panel embedded with an S-shaped wavelength shifting (WLS) fiber. The fiber is read out by two SiPMs, which are coupled to either end of the fiber and serves to transport the light over long distances with minimal attenuation. The double-ended fiber readout has the added benefit to provide some position dependence to the light generation along the panel by comparing relative signal sizes and arrival times in the two SiPMs.

The third design under consideration was motivated by increasing the attenuation length of the PD paddles and allowing collection of 400 nm photons coming from anywhere in the active volume of the TPC. The fiber-bundle design is based on a thin TPB coated acrylic radiator located in front of a close packed array of WLS fibers. This concept is designed so that roughly half of the photons converted in the radiator are incident on the bundle of fibers, the wavelength shifting fibers are Y11 UV/blue with a 4% capture probability. The fibers are then read out using SiPMs at one end. The Y11 Kuraray fibers have mean absorption and emission wavelengths of about 440 nm and 480 nm respectively. The attenuation length of the Y11 fibers is given to be greater than 3.5 m at the mean emission wavelength, which will allow production of full-scale (2 m length) photon detector paddles.

The PD system tested at the CERN neutrino platform will be based on technology selected later this year. The technology selection process will be based on a series of tests planned for the next 6 months utilizing large research cryostats at Fermilab and

Colorado State University. The primary metric used for comparison between the three technologies will be photon yield per unit cost. In addition to this metric PD threshold and reliability will also serve as inputs to the final decision. A technical panel will be assembled to make an unbiased decision.

Once the technology has been chosen the PD group will focus on optimizing the selected design with the goal of procurement and assembly taking place in late FY 2016 and early FY 2016. The photon detector paddles will then be tested and shipped to CERN in early FY 2017 for installation into the APAs in late FY 2017 in preparation for installation into the test cryostat and operation in 2018.

3.2.6 DAQ, Slow control and monitoring

The DAQ will merge data to form events from the LArTPC, photon detector and beam detector readouts using the artDAQ data acquisition toolkit using a farm of commercial computers connected with an Ethernet switch. ArtDAQ is in use on several experiments at Fermilab. We are using it on the 35t prototype, so we will have considerable experience by the time of the CERN test.

The data collection for the CERN test will operate in a mode similar to that forseen for the underground detectors. In order to collect data from non-beam interactions such as proton decay candidates or atmospheric neutrinos, data will be continuously read in to the artDAQ data receiver nodes and processed through the artDAQ system in quanta corresponding to time intervals fixed from the time of the beginning of the run. These are then transferred through the switch to a set of event building nodes which work in parallel, each node receiving all the data from all the detectors for the time intervals it is responsible for processing. There will be 32 parallel incoming data streams from the LArTPCs and 16 streams from the photon detectors. There will be an additional stream from the trigger board (the same board as built by Penn for the 35t test will be used) which will receive input of the spill gate, warning of extraction, and pattern-unit bits from trigger counters and other beamline instrumentation such as Cerenkov counters [Which section are these described in?, should we refer to them from here?].

Synchronisation across all the input sources is essential in order that artDAQ can bring together the data from the input streams correctly for processing by the event building nodes. The data receiver nodes will provide overlap by repeating the data at the boundaries of the time intervals so that a particle whose data spans two time intervals can be collected. The time synchronisation is provided to the RTM back-module on the LArTPC readout crates, to the SSP photon detector readout and to the trigger board from a GPS based time synchrononisation distribution system originally designed for the NOvA experiment. This system includes functionality to calibrate and correct for the cable delays, and to send synchronisation control signals to the readout at predetermined times.

The event building nodes will select time regions of interest within the time intervals they are processing and form these into events to be written to disk. The algorithms to select the events may be as simple as looking for a trigger bit in the trigger board data stream, or may involve looking for self-triggered events in the LArTPC data. An aggregation task, which is part of artDAQ will handle the parallelized event building processes by merging the output events into a single stream and writing them to disk. To

avoid oversized output data files, when a predetrmined file size is reached, the aggregator will switch to writing to a new file. The collaboraion requests to CERN, data links of sufficient bandwidth to transfer these files from the CENF to the CERN data center, and from there to locations worldwide for analysis.

Improved versions of the software systems which are being prototyped at the 35t test will available for the CERN test including (a) Run control which controls and monitors the DAQ processes and allows run starts and stops to be performed by the operator (b) online monitoring (c) slow control of voltages and temperatures being used by the electronics (this may not be comprehensive by the time of the CERN protoype, but we plan on prototyping the readout of some of the quantities). The trigger board includes facilities for generating calibration pulses and for identifying the event times of the calibration events.

3.2.7 Installation

The interior of the cryostat will be prepared prior to the installation of the TPC. A series of I-beam support rails will be suspended below the top surface of the cryostat membrane by a series of hangers. These hangers will be structurally supported by an independant structure above the cryostat. Decoupling the TPC support from the cryostat structure eliminates the movement of the TPC with the flexure of the cryostat structure from the filling and internal pressure changes of the Argon inside. The hangers will pass through the top of the cryostat to the independant structure inside a bellows type feed thru. These feed thrus need to be designed to minimize the heat gain into the cryogenic volume. For the CPAs, the support rails and hangers need to be electrically isolated due to high voltage concerns. To preserve the ability to reverse the order of the TPC components, all of the support points will be designed to the maximum set of requirements regarding loads and clearances.

There will be a series of feed thru flanges located along each of the support rails. These will be cryogenic flanges where the services for the TPC components can pass through the top of the cryostat. It is foreseen that each CPA row will require one feed thru for the high voltage probe to bring in the drift voltage. The drift voltage is 500 V/cm. For a drift distance of 2.5m and 3.6m, the probe voltages will be 125kV and 180kV respectively. There will be one service feed thru for each of the APAs. These feed thrus will include high speed data, bias voltages for the wire planes, control and power for the cold electronics.

The main TPC components will be installed through large hatches in the top of the cryostat. This is similar to the installation method intended for the detector at the far site. These hatches will have an aperture approximately 2.0 m wide and 3.5 m long. Each APA and CPA panel will be carefully tested after transport into the clean area and before installation into one of the cryostats. Immediately after a panel is installed it will be rechecked. The serial installation of the APAs along the rails means that removing and replacing one of the early panels in the row after others are installed would be very costly in effort and time. Therefore, to minimize the risk of damage, as much work around already installed panels as possible will be completed before proceeding with further panels. The installation sequence is planned to proceed as follows:

1. Install the monorail or crane in the staging area outside the cryostat, near the

equipment hatch.

2. Install the relay racks on the top of the cryostat and load with the DAQ and power supply crates.
3. Dress cables from the DAQ on the top of the cryostat to remote racks.
4. Construct the clean-room enclosure outside the cryostat hatch.
5. Install the raised-panel floor inside the cryostat.
6. Insert and assemble the stair tower and scaffolding in the cryostat.
7. Install the staging platform at the hatch entrance into the cryostat.
8. Install protection on (or remove) existing cryogenics instrumentation in the cryostat.
9. Install the cryostat feedthroughs and dress cables inside the cryostat along the support beams.
10. Install TPC panels:
    (a) Install the CPA panels supported from the center support rail. These will be installed from the floor of the cryostat. Access to the top edge will be required by scaffolding.
    (b) Install and connect HV probe for the CPAs.
    (c) Perform electrical tests on the connectivity of the probe to the CPAs.
    (d) Install first end wall of vertical field cage at the non-access end of the cryostat. These will be installed from the floor of the cryostat. Scaffolding will be needed to install the supporting structure and then attach the panels to the structure.
    (e) Test the inner connections of the field cage panels.
    (f) Install the first APA and connect to the far end field cage support.
    (g) Connect power and signal cables. This will require scaffolding to access the top edge of the APA.
    (h) Test each APA wire for expected electronics noise. Spot-check electronics noise while cryogenics equipment is operating.
    (i) Install the upper field cage panels for the first APA between the APA and CPAs This will require scaffolding to access the upper edge of the APA, CPA and field cage structure.
    (j) Perform electrical tests on upper field cage panels.
    (k) Repeat steps (f) through (j) for the next five APAs.
    (l) Install the lower field cage panels between the APAs and CPAs. Start at the far end away from the access hatch and work towards the hatch.

(m) Perform electrical test on lower field cage panels and the entire loop around the TPC.

(n) Remove temporary floor sections as the TPC installation progresses.

(o) Install sections of argon-distribution piping as the TPC installation progresses.

(p) Install the final end wall of vertical field cage at the access end of the cryostat. These will be installed from the floor of the cryostat. Scaffolding will be needed to install the supporting structure and then attach the panels to the structure.

11. Remove movable scaffold and stair towers.

12. Temporarily seal the cryostat and test all channels for expected electronics noise.

13. Seal the access hatch.

14. Perform final test of all channels for expected electronics noise.

In general, APA panels will be installed in order starting with the panel furthest from the hatch side of the cryostat and progressing back towards the hatch. The upper field cage will be installed in stages as the installation of APAs and CPA progresses. After the APAs are attached to the support rods the electrical connections will be made to electrical cables that were already dressed to the support beams and electrical testing will begin. Periodic electrical testing will continue to assure that nothing gets damaged during the additional work around the installed APAs.

The TPC installation will be performed in three stages, each in a separate location; the locations, or zones. First, in the clean room vestibule, a crew will move the APA and CPA panels from storage racks, rotate to the vertical position and move them into the cryostat. Secondly, in the panel-staging area immediately below the equipment hatch of the cryostat, a second crew will transfer the panels from the crane to the staging platform, where the crew inside the cryostat will connect the to the rails within the cryostat. A third crew will reposition the movable scaffolding and use the scaffold to make the mechanical and electrical connections at the top for each APA and CPA as they are moved into position.

The requirements for alignment and survey of the TPC are under development. Since there are many cosmic rays in the surface detector and beam events, significant corrections can be made for any misalignment of the TPC. The current plan includes using a laser guide or optical transit and the adjustment features of the support rods for the TPC to align the top edges of the APAs in the TPC to be straight, level and parallel within a few mm. The alignment of the TPC in other dimensions will depend on the internal connecting features of the TPC. The timing of the survey will depend on understanding when during the installation process the hanging TPC elements are in a dimensionally stable state. The required accuracy of the survey is not expected to be more precise than a few mm.

4 Cryostat and cryogenics system [~5 pages; David/Barry/Jack

4.1 Cryostat

The Single Phase TPC test at CERN will use a membrane tank technology to contain 673 tons of LAr, equivalent to about $483m^3$. The design is based on a scaled up version of the LBNE 35-ton Prototype [4] and the Fermilab Short-Baseline Near Detector [5]. The cryostat will use a steel outer supporting structure with a metal liner inside to isolate the insulation volume, similar to the one of the dual phase detector prototype WA105 $1 \times 1 \times 3$ and to the Fermilab Short-Baseline Near Detector. The support structure will rest on I-beams to allow for air circulation underneath in order to maintain the temperature within the allowable limits. This section describes the proposed design, whose scope encompasses the following components:

- steel outer supporting structure,
- main body of the membrane cryostat (sides and floor),
- top cap of the membrane cryostat.

A membrane cryostat design commonly used for liquefied natural gas (LNG) storage and transportation will be used. In this vessel a stainless steel membrane contains the liquid cryogen. The pressure loading of the liquid cryogen is transmitted through rigid foam insulation to the surrounding outer support structure, which provides external support. The membrane is corrugated to provide strain relief resulting from temperature related expansion and contraction. The vessel is completed with a top cap that uses the same technology.

Two membrane cryostat vendors are known: GTT (Gaztransport & Technigaz) from France and IHI (Ishikawajima-Harima Heavy Industries) from Japan. Each one is technically capable of delivering a membrane cryostat that meets the design requirements for this detector. To provide clarity, only one vendor is represented in this document, GTT; this is for informational purposes only. Figure 1 shows a 3D model of the GTT membrane and insulation design.

The conceptual proposed design for the Single Phase Test at CERN cryostat is a rectangular vessel measuring 8.8 m in length (parallel to the beam direction), 7.8 m in width, and 8.0 m in height; containing a total mass of 673 tons of liquid argon. Figure 14 shows side and end views of the cryostat respectively. Figure 15 shows a 3D view. To minimize the contamination from warm surfaces, during operation the temperature of all surfaces in the ullage shall be lower than 100 K. The top plate will contain two hatches for the installation of the TPCs; it will also contain a manhole to enter the tank after closing the hatches, and several penetrations for the cryogenic system and the detector.

Design Parameters

This design includes technical solutions that may be of interested for the future needs of the Long Baseline Neutrino program. For example the use of a cold ullage (<100 K) to lower the impurities in the gas region, and of a LAr pump outside the cryostat to minimize the effect of noise, vibration and microphonics to the TPC inside the liquid argon volume.

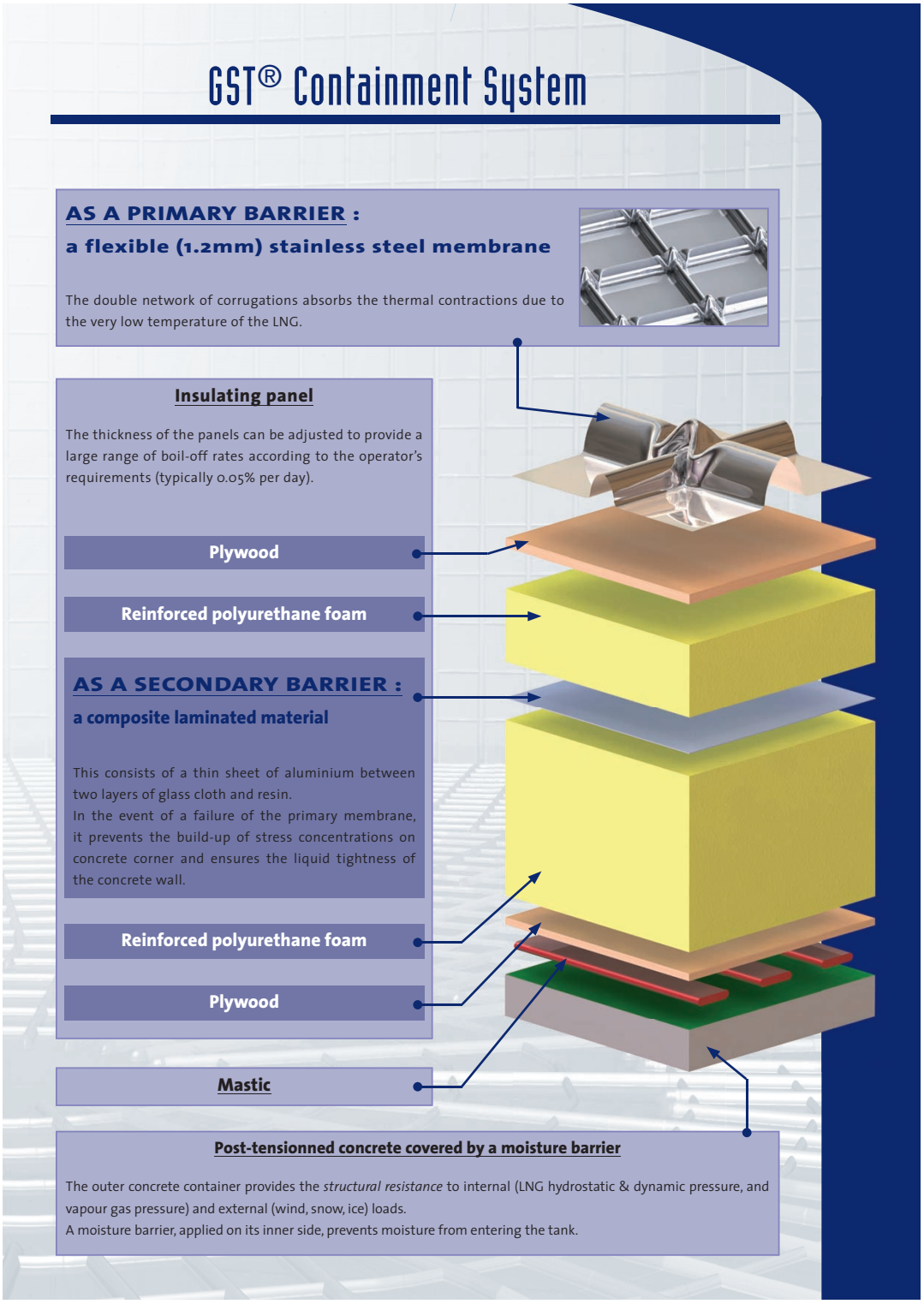

Figure 12: Exploded view of the membrane cryostat technology

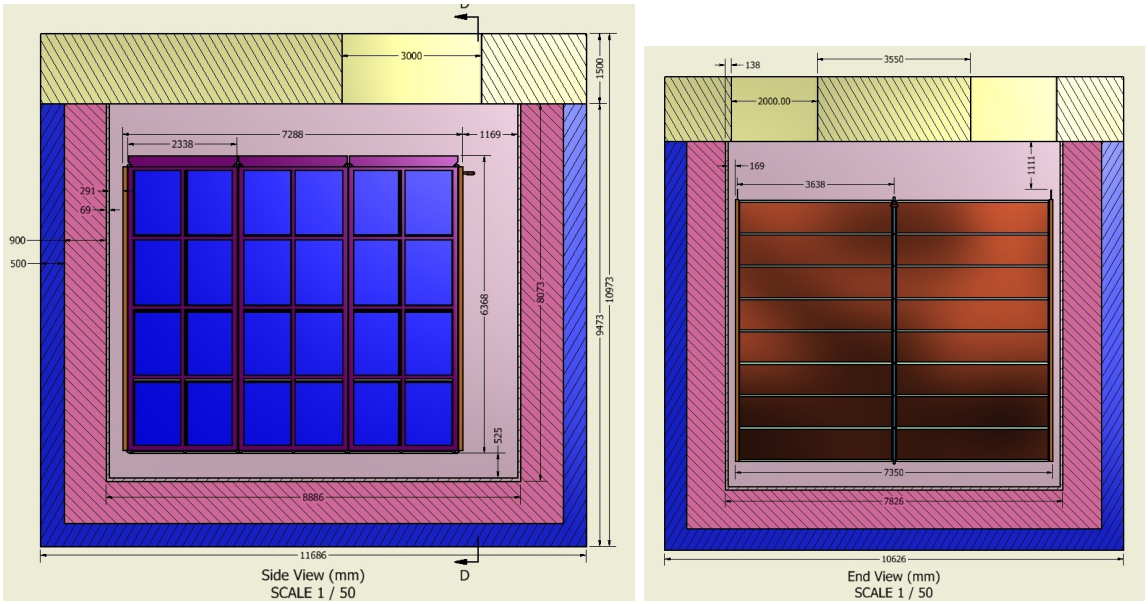

Figure 13: Side (left) and end (right) views of cryostat

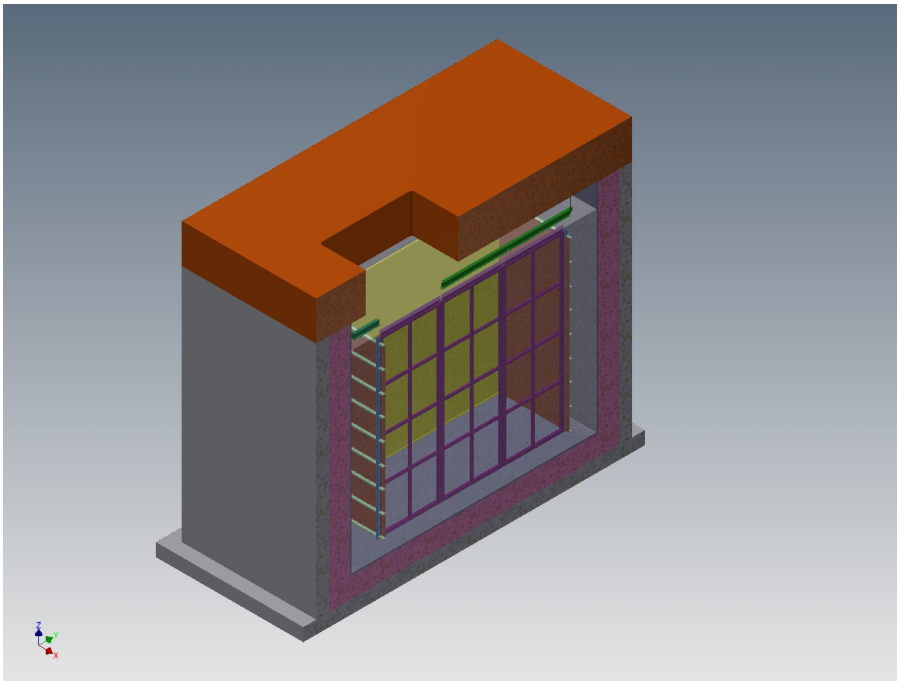

Figure 14: Isometric view of the membrane cryostat

Table 4: Design requirements for the membrane cryostat

Design Parameter	**Value**
Type of structure	Membrane cryostat
Membrane material	SS 304/304L, 316/316L or equivalent.
Fluid	Liquid argon (LAr)
Other materials upon approval.	
Outside reinforcement (support structure)	Steel enclosure with metal liner to isolate the outside from the insulation space, standing on legs to allow for air circulation underneath.
Total cryostat volume	538 m3
Total LAr volume	483 m3
LAr total mass	673,000 kg
Minimum inner dimensions (flat plate to flat plate).	7.8 m (W) x 8.8 m (L) x 8.4 0 (H)
Depth of LAr	7.2 m (0.82 m ullage, same as LBNF)
Primary membrane	1.2 mm thick SS 304L corrugated stainless steel
Secondary barrier system	GTT design; 0.07 mm thick aluminum between fiberglass cloth. Overall thickness 1 mm located between insulation layers.
Insulation	Polyurethane foam (0.9 m thick from preliminary calculations)
Maximum static heat leak	10 W/m2
LAr temperature	88 +/- 1K
Operating gas pressure	Positive pressure. Nominally 70 mbarg ($\sim$1 psig)
Vaccuum	No vacuum
Design pressure	350 mbarg ($\sim$5 psig) + LAr head (1,025 mbarg)
Design temperature	77 K (liquid nitrogen temperature for flexibility)
Temperature of all surfaces in the ullage during operation	<100 K
Leak tightness	$1e-6$ mbar*l/sec
Maximum noise/vibration/microphonics inside the cryostat	LAr pump outside the cryostat
Beam window	Precise location TBD. Figure 14 shows the location where the beam enters the cryostat.
Accessibility after operations	Capability to empty the cryostat in 30 days and access it in 60 days after the end of operations.
Lifetime / Thermal cycles	Consistent with liquid argon program. TBD.

The design parameters for the TPC Test at CERN cryostat are listed in Table 4.

Insulation system and secondary membrane

The membrane cryostat requires insulation applied to all internal surfaces of the outer support structure and roof in order to control the heat ingress and hence required refrigeration heat load. To avoid bubbling of the liquid Argon inside the tank, the maximum static heat leak is $10W/m^2$ for the floor and the sides and $15W/m^2$ for the roof, higher to account for the penetrations that increase the heat budget. Preliminary calculations show that these values it can be obtained using 0.9 m thick insulation panels of polyurethane foam. Given an average thermal conductivity coefficient for the insulation material of 0.0283 W/(m·K), the heat input from the surrounding steel is expected to be about 3.2 kW total. It assumes that the hatches are foam insulated as well. This is shown in Table 5.

The insulation material is a solid reinforced polyurethane foam manufactured as composite panels. The panels get laid out in a grid with 3 cm gaps between them (that will be filled with fiberglass) and fixed onto anchor bolts anchored to the support structure. The composite panels contain the two layers of insulation with the secondary barrier in between. After positioning adjacent composite panels and filling the 3-cm gap, the secondary membrane is spliced together by epoxying an additional overlapping layer of secondary membrane over the joint. All seams are covered so that the secondary membrane is a continuous liner.

In the current GTT design, the secondary membrane is comprised of a thin aluminum sheet and fiberglass cloth. The fiberglass-aluminum-fiberglass composite is very durable and flexible with an overall thickness of about 1 mm. The secondary membrane is placed within the insulation space. It surrounds the bottom and sides. In the unlikely event of an internal leak from the primary membrane of the cryostat into the insulation space, it will prevent the liquid cryogen from migrating all the way through to the steel support structure where it would degrade the insulation thermal performance and could possibly cause excessive thermal stress in the support structure. The liquid cryogen, in case of leakage through the inner (primary) membrane will escape to the insulation volume, which is purged with GAr at the rate of one volume exchange per day.

Table 5: Heat load calculation for the membrane cryostat (insulation thickness = 0.9 m). (note to self: has right values)

Element	**Area** (m^2)	**K** (W/mK)	**Δ T** (K)	**Heat Input** (W)
Base	83	0.0283	205	534
End walls	153	0.0283	205	986
Side walls	172	0.0283	205	1,108
Roof	83	0.0283	205	550
Total				3,162

Cryostat Configuration

With the intent to minimize the contamination in the gas region, the ullage will be kept cold (<100 K). It has been observed in the Materials Test Stand (MTS) and the

Liquid Argon Purity Demonstrator (LAPD) at Fermilab that the outgassing is significantly reduced below 100 K [add reference]. A possible way to achieve this requirement is to spray a mist of clean liquid and gaseous argon to the metal surfaces in the ullage and keep them cold, similar to the strategy that was developed for the cool down of the LBNE 35 Ton prototype.

Outer Support Structure

The proposed design is a steel support structure with a metal liner on the inside to isolate the insulation region and keep the moisture out. This choice allows natural and forced ventilation to maintain the temperature of the steel within its limit, without the need of heating elements and temperature sensors. It reduces the time needed for the construction: the structure will be prefabricated in pieces of dimensions appropriate for transportation, shipped to the destination and only assembled in place. Fabrication will take place at the vendor's facility for the most part. This shortens the construction of the outer structure on the detector site, leaving more time for completion of the building infrastructure. If properly designed, a steel structure may allow the cryostat to be moved, should that be desired in the future.

Main body of the membrane cryostat

The sides and bottom of the vessel constitute the main body of the membrane cryostat. They consist of several layers. From the inside to the outside the layers are stainless steel primary membrane, insulation, thin aluminum secondary membrane, more insulation, and steel outer support structure with meal panels acting as vapor barier. The secondary membrane contains the LAr in case of any primary membrane leaks and the vapor barrier prevents water ingress into the insulation. The main body does not have side openings for construction. The access is only from the top. There is a side penetration for the liquid argon pump for the purification of the cryogen.

Top cap

Several steel reinforced plates welded together constitute the top cap. The stainless steel primary membrane, intermediate insulation layers and vapor barrier continue across the top of the detector, providing a leak tight seal. The secondary barrier is not used nor required at the top. The cryostat roof is a removable steel truss structure that also supports the detector. Stiffened steel plates are welded to the underside of the truss to form a flat vapor barrier surface onto which the roof insulation attaches directly. The penetrations will be clustered in the back region. The top cap will have two large openings for TPC installation, and a manhole to enter the tank after the hatches have been closed.

The truss structure rests on the top of the supporting structure where a positive structural connection between the two is made to resist the upward force caused by the slightly pressurized argon in the ullage space. The hydrostatic load of the LAr in the cryostat is carried by the floor and the sidewalls. In order to meet the maximum deflection between APA and CPA and to decouple the detector form possible sources of vibrations, the TPCs will be connected to an external bridge over the top of the plate supported on the floor of the building. Everything else within the cryostat (electronics, sensors, cryogenic and gas plumbing connections) is supported by the steel plates under the truss structure. All piping and electrical penetration into the interior of the cryostat are made through this top plate, primarily in the region of the penetrations to minimize the potential for leaks. Studs are welded to the underside of the top plate to bolt the

insulation panels. Insulation plugs are inserted into the bolt-access holes after panels are mounted. The primary membrane panels are first tack-welded then fully welded to complete the inner cryostat volume.

Table 6 presents the list of the design parameters for the top of the cryostat.

Cryostat grounding and isolation requirements

The cryostat has to be grounded and electrically isolated from the building. This section presents the list of the current grounding and isolation requirements for the cryostat. Figure 15 shows the layout of the top plate grounding.

Isolation

1. The cryostat membrane and any supporting structure, whether it is a steel structure or a concrete and rebar pour, shall be isolated from any building metal or building rebar with a DC impedance greater than 300 kΩ.

2. All conductive piping penetrations through the cryostat shall have dielectric breaks prior to entering the cryostat and the top plate.

Grounding

1. The cryostat, or "detector" ground, shall be separated from the "building" ground.

2. A safety ground network consisting of saturated inductors shall be used between detector ground and building ground.

3. Parameters TBD.

Top plate grounding

1. If the cryostat is contained within a concrete pour, the top plate shall be electrically connected to any rebar used in that pour, and the rebar shall be conductively tied at regular intervals. Parameters TBD.

2. The top grounding plate shall be electrically connected to the cryostat membrane by means of copper braid connections.

   (a) Each connection shall be at least 1.6 mm thick and 63.5 mm wide.

   (b) The length of each connection is required to be as short as possible.

   (c) The distance between one connection and the next one shall be no more than 1.25 m.

   (d) The layout can follow the profile of several pieces of insulation, but it shall be continuous.

   (e) The DC impedance of the membrane to the top plate shall be less than 1 ohm.

Leak prevention

The primary membrane will be subjected to several leak tests and weld remediation, as necessary. All (100%) of the welds will be tested by an Ammonia colorimetric leak test (ASTM E1066-95) in which welds are painted with a reactive yellow paint before

Table 6: Design parameters for the top of the cryostat

Design Parameter	**Value**
Configuration	Removable metal plate reinforced with trusses/I-beams anchored to the membrane cryostat support structure. Contains multiple penetrations of various sizes and a manhole. Number, location and size of the penetrations TBD. The hatches shall be designed to be removable. If welded, provisions shall be made to allow for removal and re-welding six (6) times.
Plate/Trusses non-wet material	Steel if room temperature. SS 304/304 or equivalent if at cryogenic temperature
Wet material	SS 304/304L, 316/316L or equivalent. Other materials upon approval.
Fluid	Liquid argon (LAr)
Design pressure	350 mbarg (5 psig)
Design temperature	77 K (liquid nitrogen temperature for flexibility)
Inner dimensions	To match the cryostat
Maximum allowable roof deflection	0.003 m (differential between APA and CPA)
Maximum static heat leak	<15 W/m2
Temperatures of all surfaces in the ullage during operation	<100 K
Additional design loads	- Top self-weight - Live load (488 kg/m2) - Electronics racks (400 kg in the vicinity of the feed through) - Services (150 kg on every feed through)
TPC anchors	Number and location TBD. Minimum 6. xc
Hatch opening for TPCs installation	3.550 m x 2.000 m (location TBD)
Grounding plate	1.6 mm thick copper sheet brazed to the bottom of the top plate
Lifting fixtures	Appropriate for positioning the top at the different parts that constitute it.
Penetrations	1 LAr In, 1 Purge GAr In, 1 Vent GAr In 2 Pressure Safety Valves, 2 Vacuum Safety Valves 1 GAr boil off to condenser 1-2 Liquid level sensors 1-2 Instrumentation 1 Temperature sensors feedthroughs? 1 LAr for cool down, 1 GAr for cool down 1 TPC signal, 3 TPC feedthroughs 1 Photon Detector for APA (Cold) Calibration dc
Lifetime / Thermal cycles	Consistent with the liquid argon program TBD.

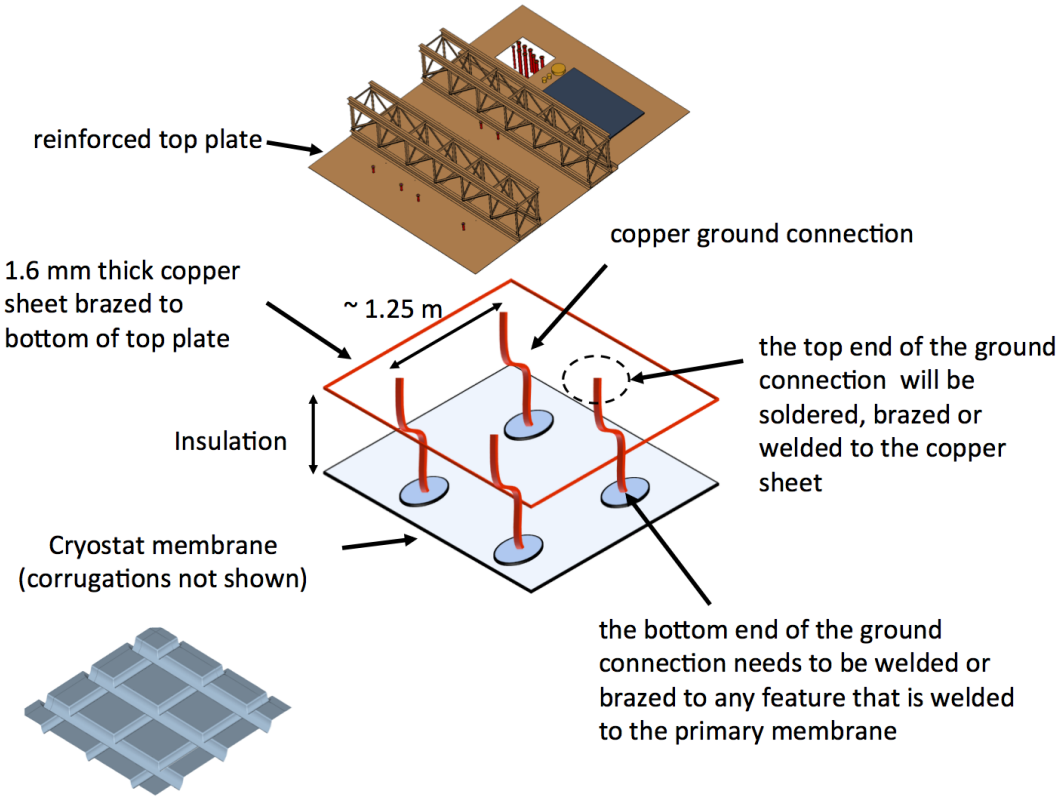

Figure 15: Top plate grounding layout

injecting a Nitrogen-Ammonia mixture into the insulation space of the tank. Wherever the paint turns purple or blue, a leak is present. The developer is removed, the weld fixed and the test is performed another time. Any and all leaks will be repaired. The test lasts a minimum of 20 hours and is sensitive enough to detect defects down to 0.003 mm in size and to a $10^{-7} std - cm^3/s$ leak rate (equivalent leak rate at standard pressure and temperature, 1 bar and 273 K). To prevent infiltration of water vapor or oxygen through microscopic membrane leaks (below detection level) the insulation spaces will be continuously purged with gaseous argon to provide one volume exchange per day. The insulation space will be maintained at 70 mbar, slightly above atmospheric pressure. This space will be monitored for changes that might indicate a leak from the primary membrane. Pressure control devices and safety relief valves will be installed on the insulation space to ensure that the pressure does not exceed the operating pressure inside the tank. The purge gas will be recirculated by a blower, purified, and reused as purge gas. The purge system is not safety- critical; an outage of the purge blower would have negligible impact on LAr purity.

4.2 Cryostat size from TPC dimensions (Move to begining of sec 4 per DM)

The minimum internal size of the cryostat is determined from size of the TPC. At the bottom of the cryostat there needs to be a minimum of 0.36 m between the frame of the CPA and closest point on the SS membrane. This is to prevent high voltage discharge between the CPA and the electrically grounded membrane. It is foreseen that there would be some cryogenic piping and instrumentation under the TPC. There is a height allowance of 0.165 m for this. There will be access and egress space around the outside of the TPC and the membrane walls. On two sides, 0.15 m of space is reserved for this. The front will have 0.36 mm and the back, where piping and instrumentation for the cryogenic system will be located, 1.20 m.

The support system for the TPC will be located outside the cryostat roof, with a bridge connected to the floor. It is the same design solution currently looked at for the DUNE TPC in the LBNF cryostat. The plan is to model this space similar to what is planned for the far site TPC. There will be 0.82 m of ullage space. In order to prevent high voltage discharge, the upper most part of the CPA needs to be submerged a minimum of 0.5 m below the liquid Argon surface. The top of the TPC will be separated from the membrane by a minimum of 1.1 m.

Adding all of these to the size of the TPC yields the minimum inner dimensions of the cryostat. A minimally sized cryostat would be 8.8m long, 7.8 m wide and 8.0 m high. This assumes the TPC will be positioned inside the cryostat with the CPAs and end field cages parallel to the walls of the cryostat. Also there is no space allotted for a beam window to enter the cryostat. Clearance would need to be added if it violates any of the current boundaries listed above. The current plan is to have the CPAs located in the center of the cryostat with an APA on each side.

4.3 Cryogenic System

Figure 16 outlines the basic scheme of the LN2 supply system, which was proposed by CERN for the Short Baseline Program and found to be an appropriate solution for this detector as well. The experiment will rely on LN2 tankers for regular deliveries to a local dewar storage, which will be sized to provide several days of cooling capacity in the event of a delivery interruption. From the dewar storage the LN2 is then transferred to a distribution facility located in the experimental hall. It includes a small buffer volume and an LN2 pumping station that transfers the LN2 to the argon condenser and other services as needed. The low estimated heat leak of the vessel ($\sim$3.2 kW) and the location inside an above ground building allow for use of an open loop system typical of other installations operated at Fermilab (LAPD, LBNE 35 ton prototype, MicroBooNE) and at CERN (???). Main goal of the LN2 system is to provide cooling power for the argon condenser, the initial cool down of the vessel and the detector, and all other services as needed.

Table 7 presents the list of requirements for the cryogenic system for the Single Phase TPC test at CERN detector.

Figure 17 shows a schematic diagram of the proposed liquid argon system. It is based on the design of the LBNE 35 ton prototype, the MicroBooNE detector systems and the current plans for the Long Baseline Far Detector.

Main goal of the LAr system is to purge the cryostat prior to the start of the operations (with GAr in open and closed loop), cool down the cryostat and fill it with LAr. Then continuously purify the LAr and the boil off GAr to maintain the required purity (electron lifetime measured by the detector).

The LAr receiving facility includes a storage dewar and an ambient vaporizer to deliver LAr and GAr to the cryostat. The LAr goes through the liquid argon handling and purification system, whereas the Gar through the gaseous argon purification before entering the vessel.

The LAr purification system is currently equipped with a filter containing mol sieve and copper beds, and a regeneration loop to regenerate the filter itself. Filters containing Oxysorb and Hydrosorb rather than mol sieve and copper beds, were also successfully employed. Same concept, but different medium. Studies are ongoing to standardize the filtration scheme and select the optimal filter medium for all future generation detectors, including this test prototype.

During operation, an external LAr pump circulates the bulk of the cryogen through the LAr purification system. The boil off gas is first recondensed and then is sent to the LAr purification system before re- entering the vessel.

Table 7: Design requirements for the cryogenic system

Parameter	**Value**
Location	Preferably not in front of the cryostat (on the beam)
Cooling Power	TBD based on the heat leak of the cryostat (estimated 3.4 kW), the cryo-piping and all other contributions (cryogenic pumps, etc.)
Liquid argon purity in cryostat	10 ms electron lifetime (30 ppt O2 equivalent)
Gaseous argon piston purge rate of rise	1.2 m/hr
Membrane cool-down rate	From manufacturer
TPCs cool-down rate	<40 K/hr,<10 K/m (vertically)
Mechanical load on TPC	The LAr or the gas pressure shall not apply a mechanical load to the TPC greater than 200 Pascal.
Nominal LAr purification flow rate (filling/ops)	5.5 day/volume exchange
Temperature of all surfaces in the ullage during operations	<100 K
Gaseous argon purge within insulation	1 volume change /day of the open space between insulation panels.
Lifetime of the cryogenic system	Consistent with the LAr program. TBD.

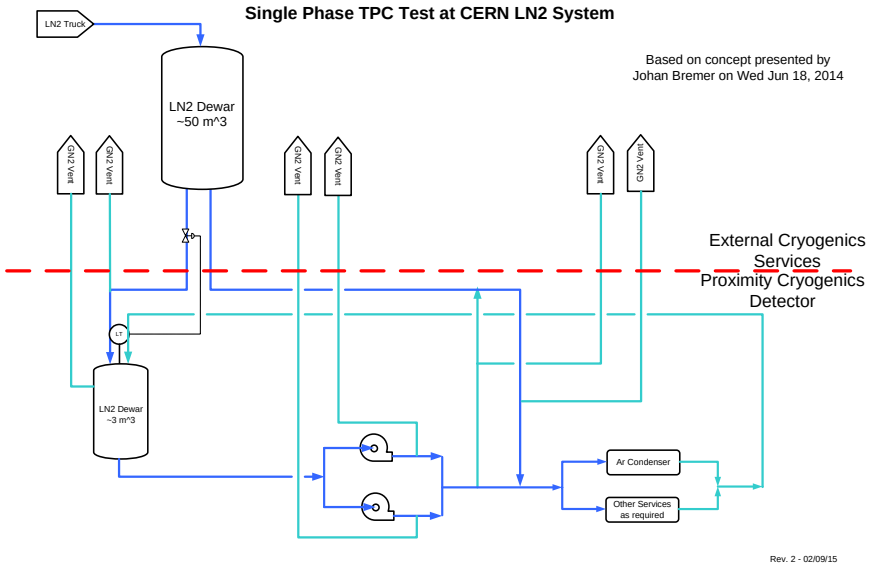

Figure 16: Schematic diagram for the proposed LN2 system

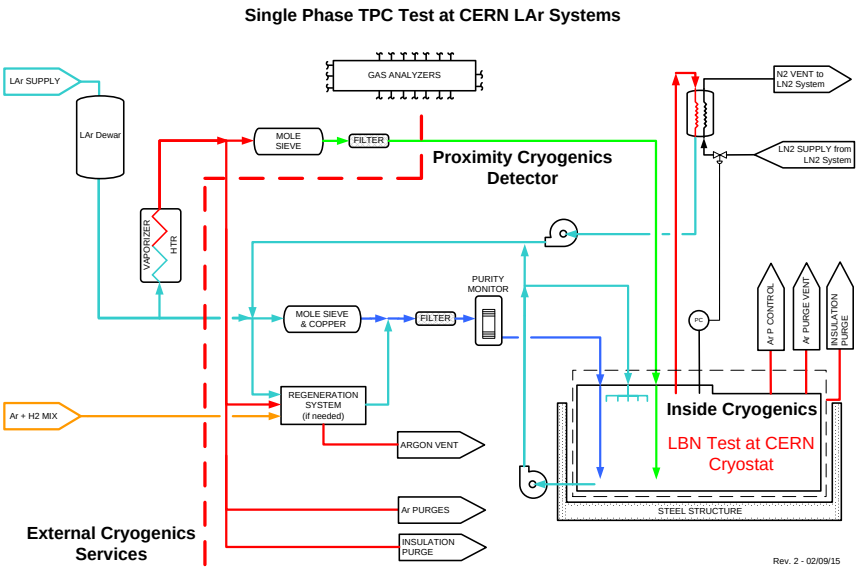

Figure 17: Schematic diagram for the proposed LAr system

5 Charged Particle Test Beam Requirements [~10 pages; Cheng-Ju]

5.1 Particle Beam Requirements

The requested beam parameters are driven by the requirement that the results from the CERN test beam should be directly applicable to the future large underground single-phase LAr detector with minimal extrapolation. The CERN test beam data will be used to evaluate the detector performance, to understand the various physics systematic effects, and to provide "neutrino-like" data for event reconstruction studies. To satisfy the requirement, the beam parameters must span a broad range of particle spectrum that are expected in the future neutrino experiment. The particle beam composition should consist of electrons, muons, and hadron beams that are charge-selected. The expected momentum distributions for secondary particles from neutrino interactions are shown earlier in Figure 2.1. There is a large spread in the momentum distribution with most particles peaked near 200 MeV/c. To cover the momentum range of interest, the momentum of the test beam should step from 0.1 GeV/c to 10 GeV/c. The maximum electron drift time in the TPC is about 3 ms. To minimize pile-up in the TPC, the desired beam rate should be around 200 Hz with the maximum rate below 300 Hz. The single-phase TPC consists of two drift volumes. It is desirable to aim the particle beam so that the hadronic showers are mostly contained in the same drift volume. However, we also plan to take some data with hadronic shower crossing the midplane of the TPC from one drift volume to another. The two beam entry angles and positions with respect to the LAr cryostat are shown in Figures 18 and 19. The beam nominally enters the cryostat slightly downward at an angle of about 6 degrees. Along the horizontal plane, the beam enters the cryostat with an angle of 10 degrees. Another possible orientation

(not shown in the Figures) to study APA crossers is to reverse the angle of the beam instead of shifting the beam parallel to the primary orientation. The summary of the beam requirements are shown in Table 8.

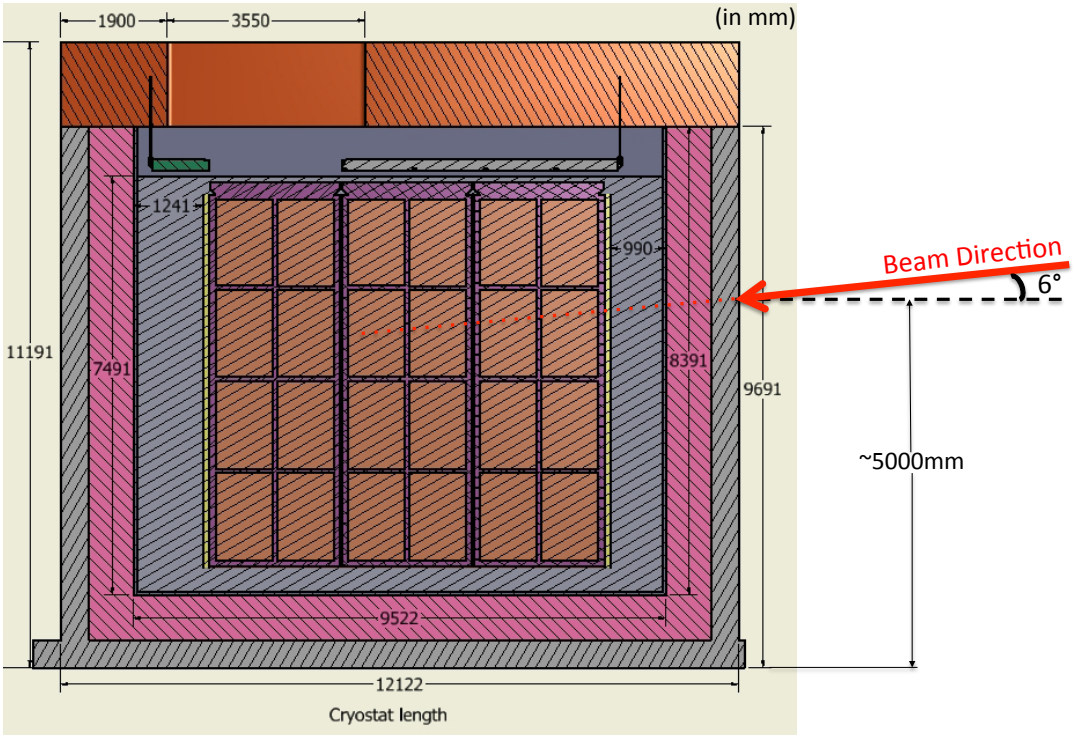

Figure 18: Side view: beam enters the cryostat slightly downward with a dip angle of 6 degrees.

5.2 EHN1 H4ext Beamline

The H4ext is an extension of the existing H4 beamline in Experimental Hall North 1 (EHN1). To produce particles in the momentum range of interest, 60 - 80 GeV/c pion beam from the T2 target is used to generate tertiary beams. The tertiary particles are momentum and charge-selected and transported down H4ext beamline to the experimental area. A preliminary layout of the H4ext beamline is shown in Figure 20.

5.2.1 Beam Optics

[Waiting for inputs from Ilias]

5.2.2 Expected Rates and Purity

[Waiting for inputs from Ilias]

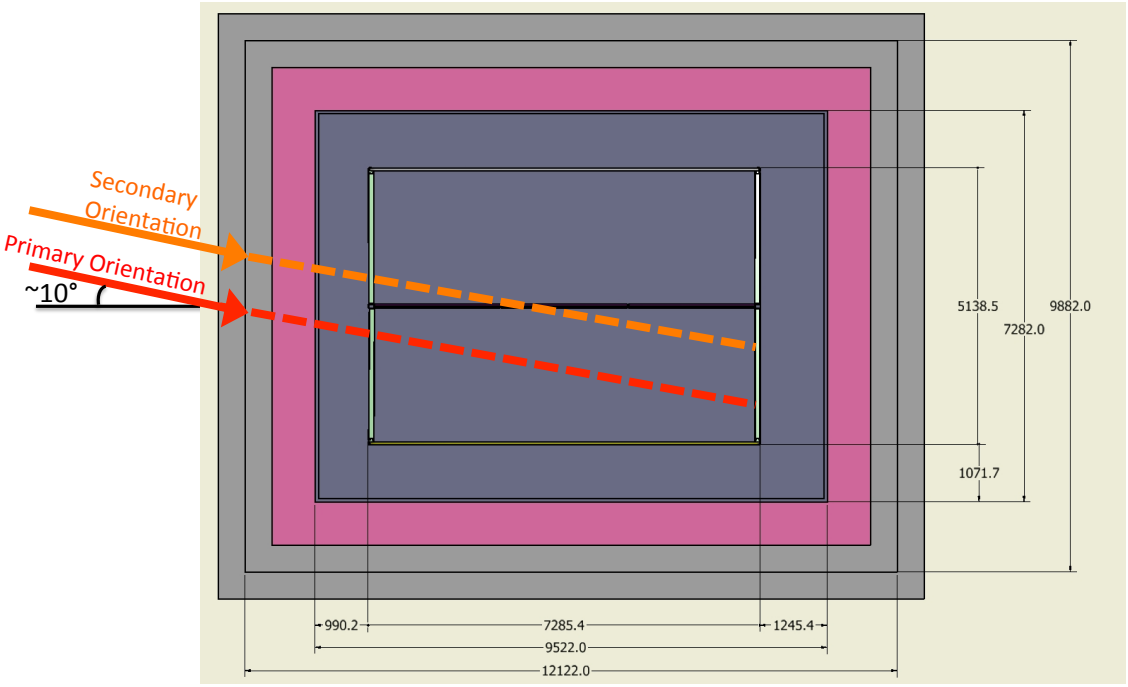

Figure 19: Top view: beam enters the cryostat with an entry angle of about 10 degrees along the horizontal plane. The primary orientation sends the particle beam into one TPC drift volume. The secondary oritentation sends the particle beam across the APA.

5.3 Beam Instrumentation

Beam instrumentation provides important information about the characteristics of the beam. It is expected that a series of detectors will be installed along the beam line to measure the particle momentum, identify particle type, and track the particle trajectory.

5.3.1 Beam Position Detector

The beam position detector measures the positions of the particle as it traverses the detector. Two detector technologies are under considerations: wire chambers and scintillating fiber trackers. For the nominal setup, one beam position detector is installed upstream and another one downstream of the last bending magnet. This pair provides additional momentum information about the particiles as well as the first set of position measurements. A third detector is placed right in front of the beam window on the cryostat wall to provide the last position information before the beam enters the cryostat.

5.3.2 Particle Identification

In order to have good particle identification over large momentum range, two indepent particle identfication systems are needed in the beamline. The Time-of-Flight system will be used to cover lower momentum range while a Threshold Cherenkov detector will be tuned for higher momentum particles.

Table 8: Particle beam requirements.

Parameter	Requirements	Notes
Particle Types	$e^{\pm}, \mu^{\pm}, \pi^{\pm}$	
Momentum Range	0.1 - 10 GeV/c	
Momentum Spread	$\Delta p/p$ <5 %	
Transverse Beam Size	RMS(x,y) < 2.5 cm	At the entrance face of the LAr cryostat
Beam Divergence		
Beam Angle (horizontal plane)	$\approx 10^{\circ}$	
Beam Dip Angle (vertical plane)	-6° (nominal); ±5° range	
Beam Entrance Position		
Rates	200 Hz (average); 300 Hz (maximum)	

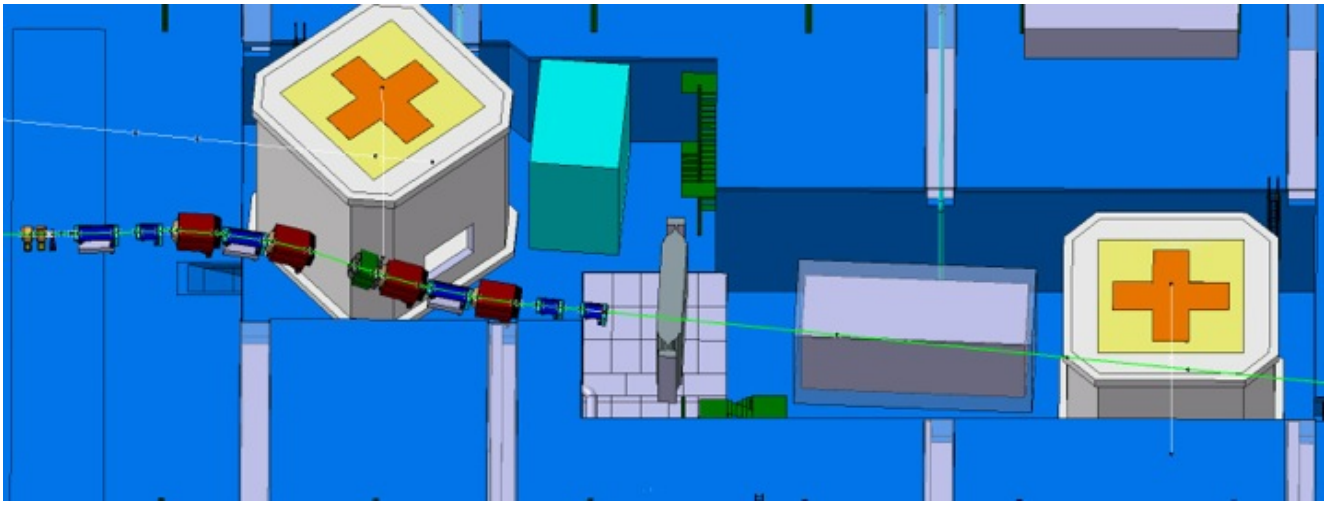

Figure 20: A conceptual layout of the H4ext beamline

5.3.3 Muon Beam Halo Counters

The halo counter is a set of plastic scintillator paddles surrounding the beamline. The main purpose is to tag particles (primarily muons from the upstream production target) that are outside of the beam axis, but may potentially enter the TPC volume. The counter information is used to either veto or simply flag these class of events.

5.4 Beam Window on LAr Cryostat

This section could be absorbed into the cryostat chapter.

6 Computing requirements, data handling and software [∼3 pages; Maxim/Craig]

6.1 Overview

The proposed "Full Scale" test of a single-phase Liquid Argon TPC at CERN will build upon the technology and expertise developed in the process of design and operation of its smaller predecessor, the 35t detector at FNAL. This includes elements of front-end electronics, data acquisition, run controls and related systems. We also expect that for the most part, Monte Carlo studies necessary to support this program will be conducted utilizing software evolved from tools currently used (2015). Likewise, event reconstruction software and analysis tools will rely on the evolving software tools developed for DUNE/LBNF.

In the test-beam setup, the detector performance will be characterized for different types of particles, e.g. p, $\pi^{\pm}$, $\mu^{\pm}$ etc (see 2.1). Current plans call for measurements in pre-defined bins of the incident particle momentum, (see Cheng-Ju's table -fixme-). The volume of the recorded data will depend on the number of events to be collected in each measurement, as specified in the run plan. As will be shown in the material presented below, cosmic ray muons have a very large impact on the data rates and volume due to the large dimensions of the TPC in this test.

In our view, it is optimal to first stage the "precious" data collected from the prototype on disk at CERN and then sink it to tape (also at CERN), while simultaneously performing replication to data centers in the US. For the latter, FNAL is the prime candidate, with additional data centers at Brookhaven National Laboratory and the NERSC facility as useful additional locations for better redundancy and more efficient access to the data from greater number of locations.

6.2 Collecting and Storing Raw Data

6.2.1 Considerations for Event Size Estimates

In addition to the sensitive volume of the TPC where Liquid Argon will serve as the active medium measuring ionization charge, the prototype will also contain a Photon Detector designed to record light pulses produced in Argon due to scintillation caused by ionizing radiation. In any realistic scenario, the amount of data to be produced by the Photon Detector will be quite small compared to that of the Liquid Argon TPC. Same goes for other elements of the experimental apparatus (hodoscopes, trigger systems etc) and as a result, for the purposes of this section, we shall focus only on the Liquid Argon TPC as the critical source of data.

To set the scale of the data generated by the TPC readout, let's consider an approximate **upper limit** on the number of channels with signals above the threshold of zero-suppression, for a single track. All numbers used in this estimate are approximate and purely for demonstration purposes. For this we assume digitization rate fixed at 2MHz, and 4312 samples per drift window. In a single anode plane assembly (APA), it will be approximately of the order of channel count in the APA, i.e. around 2500, *when the track is parallel to the APA plane*. Since each sample is 16 bit (or 12 bit in more

recent design), we arrive to the limit of approximately 20MB per single charged track. For this class of events, the amount of data will scale roughly linearly with the length of the track, i.e. in cases when a track is stopped or leaves the sensitive volume there will be less data. Further, in most cases the data will be zero-suppressed by the front-end electronics (e.g signals below a certain threshold will not be included into the outgoing data stream). The exact data reduction factor will depend on a variety of factors (cf. threshold, which is yet to be chosen), but as a rule of thumb it's an order of magnitude. *We conclude therefore the events will typically be a few megabytes in size.* In fact, this is supported by previous Monte Carlo studies performed for ealier versions of LBNE LAr TPC).

At the time of writing, work is being done on the physical design of the Liquid Argon prototype, and the number of the Anode Plane Assemblies (APA) to be installed in the detector is not yet finalized. It will likely be 2 or 3, however there is a possibility of this number to be as high as 6. There is therefore a factor of two or three uncertainty in the number of readout channels in the detector (e.g. 7680 with 3 APA vs 15360 with 6). In general, the assumption made going forward will be that the number of APAs is 6.

6.2.2 Cosmic Ray Muons

Given standard values quoted for the cosmic ray muon flux at sea level, we arrive to a number of roughly 200 incident muons per square meters per second. Taking into account the dimensions of the TPC, we estimate the area of the top face of its rectangular volume to be just over 50m^2, which means that the detector will subject to occupancy of the order of 10^4 particles per second. This is important since the drift time in liquid Argon will be of the order of 2ms, meaning that each full "frame" will contain $\sim$50 track segments on top of the actual beam event being detected. According to previous Monte Carlo studies, we will assume a ballpark value of 5MB of data to be read out per average muon track. Thus we arrive to an estimate of 250MB data load in each event, due solely to the detector exposure to cosmic rays.

6.2.3 "Before" and "After" Readout Windows

As we just mentioned, the detector will be sensitive to background tracks due to cosmic ray particles. These must be properly identified and accounted for, in order to ensure high quality of the measurements and subsequent detector characterization. Since overlay of cosmic ray muons over beam events is stochastic in nature, the optimal way to achieve this is by recording signals which were produced "just before" and "just after" the arrival of the test particle from the beamline. It will be possible because the design of the DAQ contains buffer memory that can be accessed after the trigger decision is made. This technique will enable us to record and reconstruct either partial or complete background tracks present in the "main" event.

To ensure complete collection of charge due to such tracks, the additional readout windows ("before" and "after") should equal the nominal total drift time. This will triple the amount of data due to cosmic rays, collected from the detector for each nominal event, which now translates into a total of 750MB.

6.2.4 Statistics and the Volume of Data

In view of the factors due to the cosmic ray muons presented above, the actual beam particle event data will represent but a fraction of the total volume being read out. As a concrete example, for an incident electron of 4GeV/c momentum MC calculations indicate an average event size of ∼2MB, after zero-suppression.This is less than 1% of the estimate quoted above. For that reason we will not go into the exercise of detailed estimations of the data size for each nominal class of events included in the run plan.

The run plan is presented in (see Cheng-Ju's table -fixme-). It is understood that it does not include considerations of data volume and this will be addressed below. Total statistics in the plan is approximately 25M events total, split across different particle species and insident momentum bins. Taking into account the 750MB data load per event, this leads to the estimate of the 18PB of nominal data volume to be collected in this experiment. This is obviously high and will need to be mitigated. Some of the approaches to be explored are:

- Prioritization of the run plan: the run plan may be redesigned by doing more detailed MC studies and defining priorities in a way that will allow us to reduce the statistics in certain modes of measurement

- Partial readout of the TPC: the particle beam will be narrow compared to the dimensions of the TPC. It is possible therefore to reduce the number of channels to be read out in each event.The scale of event features such as showers will determine limitations of this approach. For this readon, it is not likely that the economy will be more than a factor of ten and in practice probably less.

6.2.5 Summary of the Data Volume Estimates

The total amount of data to be collected during the prototype operation will be considerable under all assumptions and estimates. To fulfill the mission of this test beam experiment, we expect that we will need tape storage of $O(PB)$ size, and a more modest disk space for raw data staging at CERN, for replication purposes. We envisage storing the primary copy of raw data at CERN, with replicas at additional locations. There will be additional requirements for processed and Monte Carlo data placement.

6.2.6 Raw Data Transmission and Distribution

Moving data to remote locations outside of CERN is subject to a number of requirements that include:

- automation

- monitoring

- error checking and recovery (redundant checks to ensure the "precious" data was successfully sunk to mass storage at the endpoint)

- compatibility with lower-level protocols that are widespread, well uncerstood and maintained (cf. gridFTP)

There are a number of systems that can satisfy these requirements, and one of them where we possess sufficient expertise and experience is Spade, first used in IceCube [1] and then enhanced and successfully utilized in Daya Bay experiment [2].

6.3 Databases

A few types of databases will be required for the test:

- Run Log, Conditions and Slow Controls records
- Offline Calibrations

Database servers listed in the former item will need to be local to the experiment (i.e. at CERN) in order to reduce latency, improve reliability, reduce downtime dut to network outages etc. A replication mechanism will need to be put in place the data is readily available at the US and other sites. The volume of data stored in these databases will likely to be quite modest.

6.4 Software Infrastructure

Research effort within the scope of the "Full Scale" prototype at CERN will benefit from utilizing simulation toolkits, tracking and other reconstruction algorithms created in the IF community, and especially during the 35t test at FNAL.

In order to leverage this software and expertise, appropriate manpower will need to be allocated in order to create and maintain the computing infrastructure necessary for effective use of the reconstruction and physics analysis tools.

Given the widely distributed nature of the Collaboration and the need to use geographically dispersed resources (see 6.5.1), the software components of these tools will need to be portable, well maintained and validated. To ensure that this happens, we plan to establish close cooperation among participating laboratories and other research institutions.

6.5 Distributed Computing, Workload and Workflow Management

6.5.1 Distributed Processing

At the time of writing, FNAL provides the bulk of computational power for LBNE (not to mention a few other IF experiments), via Fermigrid and other facilities. We plan to leverage these resources to process the data coming from the test.

Given the relatively limited amount of beam time for this test, one of the principal goals will be quick validation of the data collected in each measurement, in order to be able to make adjustments during the run as necessary. This is a common practice in other experiment which have "express streams" to assess data quality (cf. [3]).

There are currently very large uncertainties regarding what scale of CPU power will be required to process the data, given that tracking, reconstruction and other algorithms are in a fairly early stage of development. The estimates we have at this point range

from 10 to 100 seconds required by a typical CPU to reconstruct a single event. This means that utilizing a few thousand cores through Grid facilities, it will be possible to ensure timely processing of these data.

To ensure adequate capacity, we envisage a distributed computing model where Grid resources are utilized in addition to FNAL. As an example, we have had good experience working with the Open Science Grid Consortium.

6.5.2 Scale of the Processed Data

As discussed above, we estimat the volume of raw data to be in the multi-petabyte range. We also must address the offline data, which can be classified as follows:

- Monte Carlo data, which will contain multiple event samples to cover various event types and other conditions during the measurements with the prototype detector
- Data derived from Monte Carlo events, and produced with a variety of tracking and pattern recognition algorithms in order to create a basis for the detector characterization
- Intermediate calibration files, derived from calibration data
- Processed experimental data, which will likely exist in a few brunches corresponding to a few reconstruction algorithms being applied, with the purpose of their evaluation

In the latter, there will likely be more than one processing step, thus multiplying data volume. There is sometimes a question about how much of the raw data should be preserved in the processed data streams. Given the large volume of raw data, the answer in this case will likely be "none" - for practical reasons, meaning that the derived data will be just that, and that the size of the processed data will likely by significantly smaller than the input (the raw data). Given consideration presented above, we will plan for $\sim O(1\text{PB})$ of tape storage to keep the processed data. For efficient processing, disk storage will be necessaty to stage a considerable portion of both raw data (inputs) and one or a few steps in processing (outputs).

Extrapolating from our previous experience running Monte Carlo for the former LBNE Far Detector, we estimate that we'll need a few hundred TB of continuously available disk space. In summary, we expect the need for 5PB of disk storage at FNAL to ensure optimal data availability and processing efficiency. Access to distributed data is discussed below.

6.5.3 Distributed Data

We foresee that data analysis (both experimental data and Monte Carlo) will be performed by collaborators residing in many instiurions and geographically dispersed. In our estimated above, we mostly outlined storage space requirements for major data centers like CERN and FNAL. When it comes to making these data available to the researchers, we will utilize a combination of the following:

- Managed replication of data in bulk, performed with tools like Spade discussed above. Copies will be made according to wishes and capabilities of participating institutions.

- Network-centric federated storage, based on XRootD. This allows for agile, just-in-time delivery of data to worker nodes and workstations over the network. This technology has been evolving rapidly in the past few years, and solutions have been found to mitigate performance penalty due to remote data access, by implementing caching and other techniques.

In order to act on the latter item, we plan to implement a global XRootD redirector, which will make it possible to transparently access data from anywhere. A concrete technical feature of storage at FNAL is that there is a dCache network running at this facility, with substantial capacity which can be leveraged for the needs of the CERN prototype analysis. This dCache instance is equipped with a XRootD "door" which makes it accessible to outside world, subject to proper configuration, authentication and authorization.

As already mentioned, we plan to host copies of a significant portion of raw and derived data at NERSC and also at Brookhaven National Laboratory. These two institutions have substantial expertise in the field of data handling and processing at scale and will serves as "hubs" for data archival and distribution.

7 CERN neutrino platform test environment [5 pages; David/Jack/Cheng-Ju/Thomas]

Description of Requirements, layout and constraints

We propose that the cryostat be housed in the extension of the EHN1 Bat 887 at CERN, where the cryogenic system components will also be located. (moved to sec 7)

- short description of location and orientation of cryostat + cryogenics system in EHN1 (David)

- description of beam line layout (Cheng-Ju)

- space for staging, control room, electronics racks, clean room, scaffolding, etc. (Jack)

- power requirements and cooling (Jack ?)

- ...

8 Schedule, organization and cost estimate [∼5 pages; Thomas/Greg]

8.1 Schedule

The schedule of the proposed CERN prototype detector and beam test is dictated by the ELBNF overall schedule which foresees to place the first 10 kton detector module

underground as early as calendar year 2021. Additional detector modules are expected to follow shortly thereafter. Ideally information and results from the CERN beam test will inform the decision about the final ELBNF detector design and hence should be available as soon as realistically possible. In addition, the LHC long shutdown, which is presently scheduled for mid-2018 represents a significant constraints on the schedule. In order to meet the first requirement, data taking for the initial measurement program should be complete prior to the long LHC shutdown in mid-2018. Figure 21 shows a schedule which meets this requirement. The shown schedule is based on experience of designing and manufacturing components for the 35t detector which will be commissioned starting in June 2015 at Fermilab.

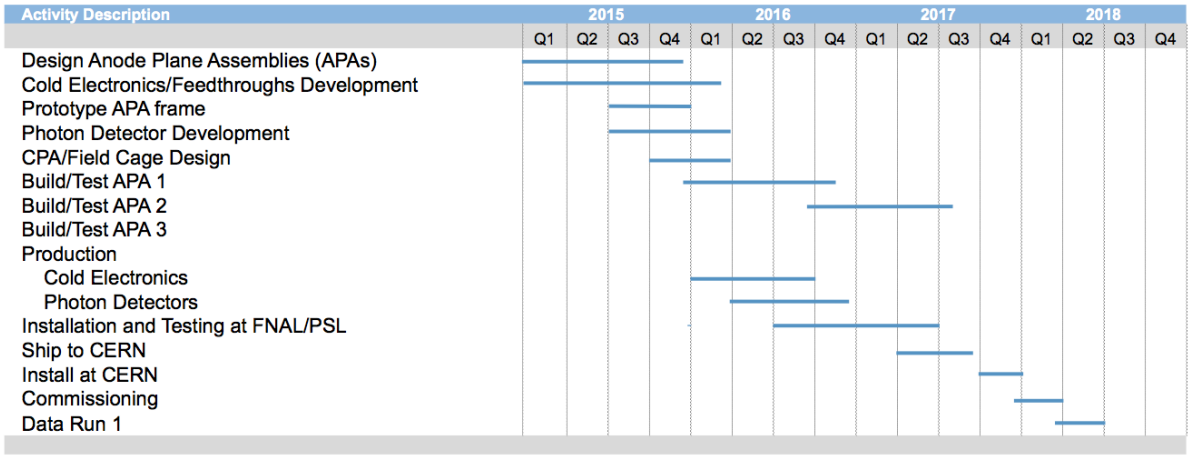

Figure 21: Rolled up version of a draft schedule for manufacturing, installing and commissioning the CERN prototype detector. A 2 - 3 months data taking period is included in the schedule.

8.2 Organization

- working group structure and distributions of tasks/responsibilities

8.3 Division of Responsibilities

8.3.1 Shared responsibilities

The engineering design of the cryostat and the cryogenics system is considered to be a shared responsibility between ELBNF and CERN.

8.3.2 ELBNF responsibilities

The following detector components are expected to be covered by ELBNF project:

1. XX APAs
2. CPA
3. field cage

4. cold electronics

5. DAQ hardware and software

6. ...

8.3.3 CERN responsibilities

The beam line design, setup of the beam line and beam monitoring instrumentation are expected to be provided by CERN.

The cryostat and cryogenics system are expected to be organized and paid for by the CERN nu-platform. The scope of the EHN1 cryostat subsystem includes the design, procurement, fabrication, testing, delivery and oversight of a cryostat to contain the liquid argon and the TPC.

The following items (incomplete list !) require further discussion. The responsibilities should be clearly spelled out.

- plans for data analysis and publications
- describe overlap/commonalities with WA105 data analysis

9 Summary [~2 pages; Thomas/Greg]

this is the summary section

References

[1] IceCube Data Movement `https://icecube.wisc.edu/science/data/datamovement`.

[2] Data processing and storage in the Daya Bay Reactor Antineutrino Experiment `http://arxiv.org/pdf/1501.06969.pdf`.

[3] Prompt reconstruction of LHC collision data with the ATLAS reconstruction software, N.Barlow et al, *Journal of Physics: Conference Series 331 (2011) 032004*

[4] First scientific application of the membrane cryostat technology, D.Montanari et al, *AIP Proceedings 1573, 1664 (2014)* `http://scitation.aip.org/content/aip/proceeding/aipcp/10.1063/1.4860907`

[5] A Proposal for a Three Detector Short-Baseline Neutrino Oscillation Program in the Fermilab Booster Neutrino Beam *R.Acciarri et al* `http://arxiv.org/abs/1503.01520`

→ total estimated page count: ~60 pages